Bloch electron spontaneous emission from a single energy band in a classical ac field

V. N. Sokolov* and G. J. Iafrate
Department of Electrical and Computer Engineering, North Carolina State University, Raleigh, North Carolina 27695-8617, USA

J. B. Krieger
Department of Physics, Brooklyn College, CUNY, Brooklyn, New York 11210, USA

(Received 18 August 2009; published 26 October 2009)

A theory for the spontaneous emission of radiation for a Bloch electron in a single superlattice (SL) energy band under the influence of an external, spatially homogeneous, classical ac electric field is presented. The classical external ac electric field is described in the vector-potential gauge. The quantum radiation field is described by the free-space quantized electromagnetic field in the Coulomb gauge. Utilizing the instantaneous eigenstates of the Bloch Hamiltonian as the basis states, the Bloch electron dynamics is described to all orders in the classical ac electric field. It is shown that the spontaneous emission occurs with frequencies equal to integral multiples of the classical ac electric field frequency; this is due to the imposition of temporal periodic motion of the Bloch electrons in the SL miniband from the external periodic ac field. From appropriately derived selection rules for photon frequency and wave-vector transitions, the total spontaneous-emission probability (TSEP) is derived to first-order perturbation theory in the quantized radiation field. A general expression is obtained for the TSEP in terms of arbitrary SL miniband parameters; further, the TSEP is analyzed in detail based on the band model for the nearest-neighbor tight-binding approximation, and results show multiharmonic behavior and ac electric field tuning properties. In the nearest-neighbor tight-binding approximation, specific results for single Bloch electron manifest distinct *plateaulike* step structure in the analysis of normalized TSEP as a function of the ratio ω_0/ω, where ω_0 is the characteristic frequency, proportional to the ac electric field amplitude, and ω is the ac electric field frequency; the plateau centers of gravity are found to be defined by the Stark delocalization condition established in ac-field transport. Further, the influence of a microcavity waveguide is established and shows enhancement as well as harmonic tuning of the TSEP due to coupling to the microcavity modal environment. Finally, the one-electron TSEP is extended, within the independent electron approximation, so as to include fractional band filling along with a constant-temperature-dependent and electron-density-dependent analysis; from this analysis, TSEP numerical estimates are projected at terahertz external field frequencies for a half-filled GaAs/AlGaAs SL miniband at zero temperature.

DOI: 10.1103/PhysRevB.80.165328 PACS number(s): 73.63.Hs, 72.10.Bg, 73.21.Cd, 73.50.Mx

I. INTRODUCTION

In the past several decades, there has been extensive interest devoted to the subject of resonant Bloch electron dynamics in narrow-band semiconductors and semiconductor superlattices (SLs) under the influence of either time-dependent[1–4] (ac) or superimposed (dc-ac) electric fields.[3,5–8] Phenomena which have been pursued for this electric field combination include electric field mediated transport, photon-assisted transport, optical absorption and emission, and Bloch electron oscillations. Moreover, the specific considerations of nonlinear optical properties in semiconductor SLs have been particularly noteworthy; the pioneering ideas of Tsu and Esaki,[9] followed by later work of others,[10–12] highlight far-infrared and terahertz nonlinearities including the manifestation of self-induced transparency. In high-frequency ac electric fields, especially in frequency ranges much higher than the characteristic frequencies for elastic- or inelastic-scattering processes, ac fields give rise to remarkable transport and optical properties such as dynamical localization and self-induced transparency. As well, in combined ac and dc electric fields, SLs can also manifest nonlinear negative conductivity which can be used to amplify radiation incident on the SL structure or generate secondary radiation from within the SL. In the work discussed here, attention is focused on the consideration of spontaneous emission (SE) of radiation emitted by a Bloch electron accelerated through a single SL miniband under the influence of a homogeneous ac electric field; here, the frequency of the ac field is assumed to be sufficiently high so that the competing elastic and inelastic processes are not considered significant in lowest order and are therefore not included in this analysis.

In the general theoretical approach for calculating the SE, use is made of a comprehensive theory developed previously by the authors[13,14] to describe Bloch electron dynamics in homogeneous electric fields of arbitrary time dependence, an approach whose strength includes the use of the vector-potential gauge for describing the external homogeneous electric field and the use of the instantaneous eigenstates of the field-dependent Bloch Hamiltonian to describe the explicit field-dependent dynamics to all orders in the external ac field; this approach has been used previously by the authors to explore a wide range of transport problems involving field-assisted transport,[15,16] optical absorption,[5] and SE of Bloch oscillations in a dc electric field.[13,14] The theoretical approach for the calculation of SE is fully quantum mechanical in that the radiation field is described as a free-space quantized electromagnetic field in the Coulomb gauge. The description of Bloch dynamics in the classical ac electric field is based on the use of instantaneous eigenstates of the field-dependent Bloch Hamiltonian. The periodicity of the ac field gives rise to the temporal Bloch electron periodic mo-

 ©2009 The American Physical Society

tion in the SL energy band; this allows the SE to be analyzed over integral multiples of the ac temporal period, showing a clear preference for maximum growth in the transition probabilities; this results in a *selection rule* yielding the photon-emission frequency as an integral multiple of classical ac-field frequency; also the resulting emitted photon wave vector is quantized as well. Using these selection rules, a general band-structure-dependent expression for total spontaneous-emission probability (TSEP) is obtained to first order in the quantized radiation field but to all orders in the classical ac field. In the nearest-neighbor tight-binding approximation for a SL miniband, the TSEP is calculated and shows multiharmonic behavior resulting in a sequence of *plateaulike* steps when displayed as a function of the ratio ω_0/ω; here ω_0 is the characteristic frequency, proportional to the ac electric field amplitude, and ω is the ac-field frequency. It is shown that the plateaulike step centers of gravity are defined by the well-known Stark delocalization condition,[1–3,7] a condition established in ac-field transport. Further, the influence of a microcavity waveguide is established and shows enhancement as well as harmonic tuning of the TSEP due to coupling to the microcavity modal environment. In the free-electron limit, the nearest-neighbor tight-binding TSEP is shown to result in emission only at the frequency of the ac field, which is essentially the well-known Thomson scattering result.[17] Lastly, the one-electron TSEP is extended, within the framework of the density-matrix method in the independent electron approximation, so as to include the description of fractional band filling and a constant-temperature dependence in the analysis; TSEP numerical estimates are presented for a half-filled miniband of a GaAs/AlGaAs SL under terahertz-frequency field conditions at zero temperature.

II. BLOCH HAMILTONIAN IN AN ELECTROMAGNETIC FIELD

The Hamiltonian for a single electron in a periodic crystal potential, $V_c(\mathbf{r})$, in a time-varying electromagnetic field can be written as

$$H = \frac{1}{2m_0}\left(\mathbf{p} - \frac{e}{c}\mathbf{A}\right)^2 + V_c(\mathbf{r}) + H_r. \tag{1}$$

Here, $\mathbf{p}$ is the momentum operator, $\mathbf{A}$ is the total vector potential consisting of $\mathbf{A}=\mathbf{A}_c+\mathbf{A}_r$, where $\mathbf{A}_c$ and $\mathbf{A}_r$ describe the external (classical) homogeneous ac electric field and the free-quantized radiation field, respectively; H_r is the Hamiltonian for the quantized radiation electromagnetic field, m_0 is the free-electron mass, e is the electron charge, c is the velocity of light in vacuum, and $\mathbf{r}$ is the spatial coordinate. In the typical classical treatment of optical absorption in solids, the classical electromagnetic ac field is taken as

$$\mathbf{E}(t) = \mathbf{E}_0 \cos(\omega t - \mathbf{K}_{ph}\cdot\mathbf{r} + \varphi), \tag{2}$$

where $\mathbf{K}_{ph}$ is the propagation wave vector of classical field "photons." Since $\mathbf{K}_{ph} \ll \mathbf{K}$, even for SLs, where $\mathbf{K}$ is the electron wave vector residing in the Brillouin zone, then the conservation of the quasimomentum of the electron-photon system essentially results in vertical transitions in $\mathbf{K}$ space once the photon wave vector is treated as negligible. Thus, in neglecting $\mathbf{K}_{ph}$ from the outset, the classical electric field becomes

$$\mathbf{E}(t) = \mathbf{E}_0 \cos(\omega t + \varphi), \tag{3}$$

a spatially homogeneous function of time alone. For a classical ac field, turned on at initial time moment $t=0$, the vector potential is $\mathbf{A}_c(t) = -c\int_0^t \mathbf{E}(t')dt' = -(c/\omega)\mathbf{E}_0[\sin(\omega t+\varphi) - \sin(\varphi)]$, where $\mathbf{E}_0$, ω, and φ are the electric field strength, frequency, and initial phase of the ac field. Letting $\mathbf{F}(t) = e\mathbf{E}(t)$ and $\mathbf{p}_c(t) = \int_0^t \mathbf{F}(t')dt'$, it then follows that $\mathbf{p}_c(t) = -(e/c)\mathbf{A}_c(t)$, that is

$$\mathbf{p}_c(t) = \frac{e}{\omega}\mathbf{E}_0[\sin(\omega t + \varphi) - \sin(\varphi)]. \tag{4}$$

In substituting the vector potential $\mathbf{A}=\mathbf{A}_c+\mathbf{A}_r$ into Eq. (1) and regarding the term containing $\mathbf{A}_r$ as a perturbation, the exact Hamiltonian of Eq. (1) can be reduced to a sum of the following separate Hamiltonians $H=H_0+H_r+H_I$.[13] Here, the first two terms represent the Hamiltonian, $H_0(t)=[\mathbf{p}+\mathbf{p}_c(t)]^2/2m_0+V_c(\mathbf{r})$, for a single electron in a periodic crystal potential $V_c(\mathbf{r})$ interacting with a homogeneous ac electric field, and the Hamiltonian, H_r, for the free-quantized radiation field $H_r=\Sigma_{\mathbf{q},j}\hbar\omega_q a^\dagger_{\mathbf{q},j}a_{\mathbf{q},j}$, where $\omega_q=cq$, the free-space photon dispersion, $\hbar$ is the reduced Planck constant, $a^\dagger_{\mathbf{q},j}$ and $a_{\mathbf{q},j}$ are the creation and annihilation boson operators of the quantum radiation field, respectively. Then, starting with the reduced Hamiltonian $H=H_0+H_r+H_I$ regarding $H_I(t)$ as a perturbation, $H_I(t)=-(e/m_0c)[\mathbf{p}+\mathbf{p}_c(t)]\cdot\mathbf{A}_r$, use is made of first-order time-dependent perturbation theory to calculate SE transitions probabilities between states of the unperturbed Hamiltonian H_0+H_r. The vector potential term, $\mathbf{A}_r$, is given as

$$\mathbf{A}_r = \sqrt{\frac{2\pi\hbar c}{V}}\sum_{\mathbf{q},j}\frac{\hat{\boldsymbol{\varepsilon}}_{\mathbf{q},j}}{\sqrt{q}}(a_{\mathbf{q},j}e^{i\mathbf{q}\cdot\mathbf{r}} + a^\dagger_{\mathbf{q},j}e^{-i\mathbf{q}\cdot\mathbf{r}}), \tag{5}$$

where $\hat{\boldsymbol{\varepsilon}}_{\mathbf{q},j}$ is a unit polarization vector for the radiation mode with wave vector $\mathbf{q}$ and polarization $j=1,2$; V is the volume of the system, and $q=|\mathbf{q}|$, the magnitude of wave vector $\mathbf{q}$. The vector potential $\mathbf{A}_r$ satisfies the Coulomb gauge, $\nabla\cdot\mathbf{A}_r=0$; then, from Eq. (5), it follows that $\hat{\boldsymbol{\varepsilon}}_{\mathbf{q},j}\cdot\mathbf{q}=0$ for each polarization direction.

III. ONE-PHOTON SPONTANEOUS-EMISSION TOTAL PROBABILITY

Consideration is given to the situation in which the electron is confined to a single band of a periodic crystal with energy $\varepsilon(\mathbf{K})$ ignoring the effects of interband coupling[15] and electron intraband scattering. For the case of one-photon SE, which assumes that initially no photons are present in the radiation field when the ac field is turned on ($t=0$), the total SE probability at a time t is given by[13]

$$P_e^s(t) = \sum_{\mathbf{q},j}|A^{(e)}_{\mathbf{q},j}(\mathbf{k}_0,t)|^2, \tag{6}$$

where time-dependent wave vector $\mathbf{k}_0(t)=\mathbf{K}_0+\mathbf{p}_c(t)/\hbar$ corresponds to the instantaneous eigenstates of the Hamiltonian

H_0, and $\mathbf{K}_0$ is the initial values of the wave vector $\mathbf{K}$. The probability amplitude for one-photon emission with wave vector $\mathbf{q}$ and polarization j is obtained as

$$A^{(e)}_{\mathbf{q},j}(\mathbf{k}_0,t) = \frac{D}{\sqrt{q}}\int_0^t dt'\mathbf{v}[\mathbf{k}_0(t')-\mathbf{q}]\cdot\hat{\boldsymbol{\varepsilon}}_{\mathbf{q},j}\exp\left\{-\frac{i}{\hbar}\int_0^{t'}\{\varepsilon[\mathbf{k}_0(t_1)] - \varepsilon[\mathbf{k}_0(t_1)-\mathbf{q}]-\hbar\omega_q\}dt_1\right\}, \tag{7}$$

where $\mathbf{v}(\mathbf{k}_0)=(1/\hbar)\nabla_{\mathbf{K}}\varepsilon(\mathbf{K})|_{\mathbf{k}_0}$ is the electron velocity, $D=-i\sqrt{2\pi\alpha/V}$, and $\alpha=e^2/\hbar c$ is the fine-structure constant.

In evaluating $A^{(e)}_{\mathbf{q},j}(\mathbf{k}_0,t)$, it is assumed that the external ac field, $\mathbf{E}$, is along the z axis, also the growth direction of a superlattice with the period a, i.e., $\mathbf{E}_0=\{0,0,E_0\}$. It then follows from Eq. (4) through the well-known[15] relation $\mathbf{F}(t)=\hbar\dot{\mathbf{k}}(t)$ that

$$k_{0z}(t) = K_{0z} + \frac{\omega_0}{a\omega}[\sin(\omega t+\varphi)-\sin(\varphi)] \tag{8}$$

and $\mathbf{k}_{0\perp}(t)=\mathbf{K}_{0\perp}=$const, where $\mathbf{k}_{0\perp}(t)$ is the component of wave vector $\mathbf{k}_0(t)$ perpendicular to the z axis and $\omega_0=eE_0a/\hbar$ is the characteristic frequency associated with the ac-field amplitude E_0. In taking advantage of the periodic properties of the terms in Eq. (7) imposed by the periodicity of the ac field, $A^{(e)}_{\mathbf{q},j}(\mathbf{k}_0,t)$ is evaluated in *clocked* integral multiples of the ac-field period, $\tau=2\pi/\omega$, so that $t=N\tau$ in Eq. (7). The periodic properties of the energy and velocity resulting from the ac field are easily seen by expressing the energy band $\varepsilon(\mathbf{K})$ in the Wannier representation,

$$\varepsilon(\mathbf{K}) = \sum_{\ell}\epsilon(\ell)e^{i\mathbf{K}\cdot\ell}, \tag{9a}$$

with the Fourier coefficients

$$\epsilon(\ell) = \frac{1}{\mathcal{N}}\sum_{\mathbf{K}}\varepsilon(\mathbf{K})e^{-i\mathbf{K}\cdot\ell}, \tag{9b}$$

where ℓ is a lattice vector and $\mathcal{N}$ is the number of lattice sites; in this representation, the Bloch electron velocity is given by

$$\mathbf{v}(\mathbf{K}) = \frac{i}{\hbar}\sum_{\ell}\ell\,\epsilon(\ell)e^{i\mathbf{K}\cdot\ell}. \tag{9c}$$

It is then easy to see the ac time dependence explicitly by putting $k_{0z}(t)$ from Eq. (8) into Eqs. (9a) and (9c). Then the renormalized energy band is expressed as

$$\varepsilon(\mathbf{k}_0) = \sum_{\ell_z}\epsilon(a\ell_z,\mathbf{K}_{0\perp})e^{i\ell_z(aK_{0z}-(\omega_0/\omega)\sin\varphi)}e^{i\ell_z(\omega_0/\omega)\sin(\omega t+\varphi)}, \tag{10a}$$

where

$$\epsilon(a\ell_z,\mathbf{K}_{0\perp}) = \sum_{\ell_\perp}\epsilon(a\ell_z,\ell_\perp)e^{i\mathbf{K}_{0\perp}\cdot\ell_\perp}. \tag{10b}$$

The renormalized Bloch electron velocity is given by

$$\mathbf{v}(\mathbf{k}_0) = \frac{i}{\hbar}\sum_{\ell}\ell\,\epsilon(\ell)e^{i[\mathbf{K}_{0\perp}\cdot\ell_\perp+\ell_z(aK_{0z}-(\omega_0/\omega)\sin\varphi)]}e^{i\ell_z(\omega_0/\omega)\sin(\omega t+\varphi)}. \tag{10c}$$

A. Selection rules for spontaneous emission of a single photon

It then follows from the periodic property of the energy band resulting from the temporal property of the ac field, and therefore the electron velocity as well, that the probability amplitude, at integral multiples of the ac-field period, can be expressed as[15]

$$A^{(e)}_{\mathbf{q},j}(\mathbf{k}_0,N\tau) = \left[\frac{1-\exp(-iN\beta_q)}{1-\exp(-i\beta_q)}\right]A^{(e)}_{\mathbf{q},j}(\mathbf{k}_0,\tau). \tag{11}$$

Here, the parameter β_q is given by

$$\beta_q = \frac{1}{\hbar}\int_0^{\tau}\{\varepsilon[\mathbf{k}_0(t)]-\varepsilon[\mathbf{k}_0(t)-\mathbf{q}]-\hbar\omega_q\}dt \tag{12}$$

and, $A^{(e)}_{\mathbf{q},j}(\mathbf{k}_0,\tau)$, the probability amplitude over a single ac-field period τ is

$$A^{(e)}_{\mathbf{q},j}(\mathbf{k}_0,\tau) = \frac{D}{\sqrt{q}}\int_0^{\tau}dt\mathbf{v}(\mathbf{k}_0-\mathbf{q})\cdot\hat{\boldsymbol{\varepsilon}}_{\mathbf{q},j}\exp\left\{-\frac{i}{\hbar}\int_0^t\{\varepsilon[\mathbf{k}_0(t_1)] - \varepsilon[\mathbf{k}_0(t_1)-\mathbf{q}]-\hbar\omega_q\}dt_1\right\}. \tag{13}$$

It is noted that this property seen in Eqs. (11) and (12) associated with summing over integral multiples of $N\tau$ to get a coherent sum of phases as a prefactor of the probability amplitude, $A^{(e)}_{\mathbf{q},j}(\mathbf{k}_0,\tau)$, over a single ac-field period, τ, is similar to the result achieved in previous work[5,13–16] involving the constant electric field, except in the previous case, the periodic condition was due to the Bloch oscillation period associated with the lattice; here the periodic condition is due to the temporal periodicity of the ac field. It then follows from Eq. (11) that

$$|A^{(e)}_{\mathbf{q},j}(\mathbf{k}_0,N\tau\,)|^2 = \frac{\sin^2(N\beta_q/2)}{\sin^2(\beta_q/2)}|A^{(e)}_{\mathbf{q},j}(\mathbf{k}_0,\tau)|^2. \tag{14}$$

From Eq. (14), it is seen that $|A^{(e)}_{\mathbf{q},j}(\mathbf{k}_0,N\tau)|^2$ will reach its maximum-growth value when $\beta_q=2\pi(m+\delta)$, where m is a positive integer and $\delta\to 0$; for this limit, the function $\sin^2(N\beta_q/2)/\sin^2(\beta_q/2)\to N^2$. This condition for maximum growth establishes the *selection rule*[13] for the photon-emission frequency and wave vector. Indeed, from the condition $\beta_q=2\pi m$, it follows from Eq. (12) that

$$\omega_q = m\omega + \frac{1}{\hbar\tau}\int_0^{\tau}[\varepsilon(\mathbf{k}_0)-\varepsilon(\mathbf{k}_0-\mathbf{q})]dt. \tag{15}$$

The second term on the right-hand side of Eq. (15) is the change in the average band energy divided by $\hbar$ incurred by the electron during the emission process. For interband transitions across a band gap, with $\varepsilon(\mathbf{k}_0)$ in one band and $\varepsilon(\mathbf{k}_0-\mathbf{q})$ in an adjacent band, this can be a sizeable term, even for

vanishingly small $\mathbf{q}$. However, for the single-band situation considered here, the second term on the right-hand side of Eq. (15) is negligibly small for nonrelativistic Bloch electron velocities;[18] thus one generally has

$$\omega_q \simeq m\omega, \quad q \simeq q_m = m\frac{\omega}{c}, \tag{16}$$

the photon-emission resonance condition.[15] With increasing N, the relative probability spectral density $\eta(\omega_q) = |A^{(e)}_{\mathbf{q},j}(\mathbf{k}_0, N\tau)|^2 / |A^{(e)}_{\mathbf{q},j}(\mathbf{k}_0, \tau)|^2$ becomes sharply peaked at the resonances because the function $y(x) = \sin^2(N\pi x)/[N\sin^2(\pi x)]$ behaves like a delta function at each $N(=1, 2, \ldots)$ as $x \to 0$. Thus, the modes depicted by the selection rules of Eq. (16) radiate with the highest probability and correspond to the fundamental ac-field frequency ω and its higher harmonics.

B. Total spontaneous-emission probability: Temperature-independent one-electron analysis

The total SE probability is evaluated from Eq. (6) with the SE-probability amplitude given in Eq. (7). The SE probability is evaluated at time $t = N\tau$ by substituting $|A^{(e)}_{\mathbf{q},j}(\mathbf{k}_0, N\tau)|^2$, already obtained in Eq. (14), into Eq. (6) to obtain

$$P^s_e \equiv P^s_e(N\tau) = \frac{V}{(2\pi)^3}\int_0^{q_{max}} dq q^2 \frac{\sin^2(N\beta_q/2)}{\sin^2(\beta_q/2)} \times \int_0^{4\pi} d\Omega \sum_j |A^{(e)}_{\mathbf{q},j}(\mathbf{k}_0, \tau)|^2. \tag{17}$$

The sum over $\mathbf{q}$ in Eq. (6) has been replaced by an integral over $\mathbf{q}$ for a single polarization such that $\Sigma_{\mathbf{q}}(\cdots) \to [V/(2\pi)^3]\int dq q^2 \int d\Omega(\cdots)$, where $d\Omega = \sin\theta d\theta d\varphi_0$ is the element of solid angle subtended by $\mathbf{q}$ and θ, φ_0 are the polar angles. Further, it is observed in the integral that the term $\frac{\sin^2(N\beta_q/2)}{\sin^2(\beta_q/2)}$ is a sharply peaked function of q at q values of $q_m = m\omega/c$, where m is an integer, as noted in Eq. (16). Thus, at every node defined by the resonance conditions, with $\omega_q/\omega = m$ and $q_m = m\omega/c$, the slowly varying function of q in the integrand $q^2\Sigma_j |A^{(e)}_{\mathbf{q},j}(\mathbf{k}_0, \tau)|^2$ can be replaced by its value evaluated at $q = q_m$, and then removed from the integral over q. The remaining term in the integrand can be evaluated as $\int dq \frac{\sin^2(N\beta_q/2)}{\sin^2(\beta_q/2)} = N\omega/c$. Thus, Eq. (17) becomes

$$P^s_e = N\frac{\omega}{c}\frac{V}{(2\pi)^3}\sum_{l=1}^{l_{max}} q_l^2 \int_0^{4\pi} d\Omega \sum_j |A^{(e)}_{\mathbf{q}_l,j}(\mathbf{k}_0, \tau)|^2, \tag{18}$$

where the upper limit l_{max} in the sum over higher harmonics of the ac-field frequency ω follows from $q_{max} = l_{max}\omega/c$.[19] The calculation of P^s_e in Eq. (18) now requires the use of $A^{(e)}_{\mathbf{q},j}(\mathbf{k}_0, \tau)$ in Eq. (13), evaluated at the maximum-growth conditions of Eq. (15) expressed in selection rules of Eq. (16). The required time integral in Eq. (13) is developed by expressing the energy band $\varepsilon(\mathbf{K})$ in the Wannier representation $\varepsilon(\mathbf{K}) = \Sigma_\ell \epsilon(\ell) e^{i\mathbf{K}\cdot\ell}$ with the Fourier coefficients given in Eq. (9b). In this representation, the Bloch electron velocity is given by Eq. (9c). In addition, the dependence upon $\mathbf{q}$ in Eq. (13) is made explicit by invoking the assumption of photon long-wavelength limit by letting $\varepsilon(\mathbf{k}_0 - \mathbf{q}) \simeq \varepsilon(\mathbf{k}_0) - \mathbf{q}\cdot\nabla_{\mathbf{k}_0}\varepsilon(\mathbf{k}_0)$ and $\mathbf{v}(\mathbf{k}_0 - \mathbf{q}) \simeq \mathbf{v}(\mathbf{k}_0) - \mathbf{q}\cdot\nabla_{\mathbf{k}_0}\mathbf{v}(\mathbf{k}_0)$. In keeping the zero-order terms in $\mathbf{q}$ only and using the selection rule of Eq. (16), $\omega_q \simeq m\omega$, the probability amplitude in Eq. (13) becomes

$$A^{(e)}_{\mathbf{q},j}(\mathbf{k}_0, \tau) = \frac{D\tau}{\sqrt{q}}\hat{\varepsilon}_{\mathbf{q},j}\cdot\langle\mathbf{v}\rangle_{m\omega}, \tag{19a}$$

where

$$\langle\mathbf{v}\rangle_{m\omega} = \frac{1}{\tau}\int_0^\tau dt \mathbf{v}[\mathbf{k}_0(t)]e^{im\omega t} \tag{19b}$$

is the temporal Fourier transform of the velocity with respect to ω; this establishes the formal relationships between the velocity transport characteristics and the SE amplitude for each harmonic. In mathematical detail, and in following the spirit of Eq. (19b), the Fourier transform of the velocity becomes

$$\langle\mathbf{v}\rangle_{\omega_q} = \frac{i}{\hbar\tau}\sum_\ell \ell\epsilon(\ell)\int_0^\tau dt e^{i[\ell\cdot\mathbf{k}_0(t) + \omega_q t]}. \tag{20}$$

It is convenient to separate polarization $\hat{\boldsymbol{\varepsilon}}_{\mathbf{q},j}$ into parallel and perpendicular components with respect to the ac-field direction (i.e., along the z axis). Letting $\ell\cdot\hat{\boldsymbol{\varepsilon}}_{\mathbf{q},j} = a\ell_z(\hat{\boldsymbol{\varepsilon}}_{\mathbf{q},j})_z + \ell_\perp\cdot(\hat{\boldsymbol{\varepsilon}}_{\mathbf{q},j})_\perp$, one finds for the parallel contribution, neglecting the perpendicular component contribution of $\hat{\boldsymbol{\varepsilon}}_{\mathbf{q},j}$ as vanishing,[20] that Eq. (19a) reduces to

$$A^{(e)}_{\mathbf{q},j}(\mathbf{k}_0, \tau) = \frac{D\tau}{\sqrt{q}}(\hat{\boldsymbol{\varepsilon}}_{\mathbf{q},j})_z\langle v_z\rangle_{\omega_q}, \tag{21a}$$

where

$$\langle v_z\rangle_{\omega_q} = \frac{i}{\hbar}\sum_{\ell_z}\epsilon(a\ell_z, \mathbf{K}_{0\perp})a\ell_z e^{i\ell_z\phi_z} I_{\ell_z,q}(\tau). \tag{21b}$$

Here, use is made of the designations

$$\epsilon(a\ell_z, \mathbf{K}_{0\perp}) = \sum_{\ell_\perp}\epsilon(a\ell_z, \ell_\perp)e^{i\mathbf{K}_{0\perp}\cdot\ell_\perp}, \tag{22a}$$

$$\phi_z = aK_{0z} - \frac{\omega_0}{\omega}\sin\varphi, \tag{22b}$$

and the time integral, $I_{\ell_z,q}(\tau)$, is given as

$$I_{\ell_z,q}(\tau) = \frac{1}{\tau}\int_0^\tau dt e^{i[\omega_q t + \ell_z(\omega_0/\omega)\sin(\omega t + \varphi)]}. \tag{23}$$

The time integral is further evaluated by noting that

$$e^{i\ell_z(\omega_0/\omega)\sin(\omega t+\varphi)} = \sum_{n=-\infty}^{\infty} J_n\left(\ell_z\frac{\omega_0}{\omega}\right)e^{in(\omega t+\varphi)}, \tag{24}$$

where $J_n(\ell_z\frac{\omega_0}{\omega})$ is a Bessel function of the first kind; by making use of the maximum-growth selection rule $\omega_q = m\omega$ as expressed in Eq. (16), it follows, while using $\tau = 2\pi/\omega$, that

$$I_{\ell_z,q_m}(\tau) = (-1)^m J_m\left(\ell_z \frac{\omega_0}{\omega}\right) e^{-im\varphi}. \tag{25}$$

Then $\langle v_z\rangle_{\omega_q=m\omega}$ from Eq. (21b) becomes

$$\langle v_z\rangle_{\omega_q=m\omega} = (-1)^m e^{-im\varphi} \frac{i}{\hbar} \sum_{\ell_z} \epsilon(a\ell_z, \mathbf{K}_{0\perp}) a\ell_z e^{i\ell_z\phi_z} J_m\left(\ell_z \frac{\omega_0}{\omega}\right). \tag{26}$$

One therefore can see that Eq. (21a) becomes

$$A^{(e)}_{\mathbf{q}_m,j}(\mathbf{k}_0,\tau) = \frac{2\pi i D}{\hbar\omega\sqrt{q_m}} (\hat{\boldsymbol{\varepsilon}}_{\mathbf{q}_m,j})_z (-1)^m e^{-im\varphi} \sum_{\ell_z} \epsilon(a\ell_z, \mathbf{K}_{0\perp}) \times a\ell_z e^{i\ell_z\phi_z} J_m\left(\ell_z \frac{\omega_0}{\omega}\right). \tag{27}$$

The result of Eq. (27) is valid for a *general band structure* and may be used in Eq. (18) for the analysis of the TSEP depending on the specific band-structure characteristics. But for the nearest-neighbor tight-binding band model, when $\ell_z = 0, \pm 1$ only must be considered in the sum over ℓ_z, Eq. (27) is considerably simplified. This will be presented in the next section.

C. Results for nearest-neighbor tight-binding band model

In the nearest-neighbor tight-binding model, the electron energy dispersion is expressed as

$$\varepsilon(\mathbf{K}) = \varepsilon(0) + \Delta \sin^2\frac{aK_z}{2} + \varepsilon_\perp(\mathbf{K}_\perp), \tag{28}$$

where $\varepsilon(0)$ and Δ are the miniband edge and width, respectively, and $\varepsilon_\perp(\mathbf{K}_\perp)$ is the contribution from the perpendicular components of the band. Also, for this energy band, it follows that $\epsilon(a,\mathbf{K}_{0\perp}) = -\Delta/4$ and $\epsilon^*(a\ell_z,\mathbf{K}_{0\perp}) = \epsilon(-a\ell_z,\mathbf{K}_{0\perp})$, and $v_{max} = a\Delta/2\hbar$ is the maximum velocity in the band. Thus, the probability amplitude in Eq. (27) becomes

$$A^{(e)}_{\mathbf{q}_m,j}(\mathbf{k}_0,\tau) = \frac{2\pi i D}{\omega\sqrt{q_m}} v_{max} (\hat{\boldsymbol{\varepsilon}}_{\mathbf{q}_m,j})_z e^{-im\varphi} \Phi_m(\omega_0/\omega, \phi_z), \tag{29}$$

where the function $\Phi_m(\omega_0/\omega, \phi_z)$ is defined separately for even $(m=2k)$ harmonics as

$$\Phi_{m=2k}(\omega_0/\omega, \phi_z) = -iJ_{2k}(\omega_0/\omega)\sin\phi_z \tag{30a}$$

and for odd $(m=2k+1)$ harmonics,

$$\Phi_{m=2k+1}(\omega_0/\omega, \phi_z) = J_{2k+1}(\omega_0/\omega)\cos\phi_z. \tag{30b}$$

We note that the Fourier transform of the velocity z component is expressed as

$$\langle v_z\rangle_{m\omega} = iv_{max} e^{-im\varphi} \Phi_m(\omega_0/\omega, \phi_z), \tag{31}$$

where absolute value squared is expressed as

$$|\langle v_z\rangle_{m\omega}|^2 = v^2_{max} |\Phi_m(\omega_0/\omega, \phi_z)|^2. \tag{32}$$

The probability amplitude of Eq. (29) can now be utilized in Eq. (18) to obtain

$$|A^{(e)}_{\mathbf{q}_l,j}(\mathbf{k}_0,\tau)|^2 = 8\pi^3\alpha \frac{v^2_{max}}{\omega^2 q_l V} |(\hat{\boldsymbol{\varepsilon}}_{\mathbf{q}_l,j})_z|^2 |\Phi_l(\omega_0/\omega, \phi_z)|^2. \tag{33}$$

In making use of Eq. (33) in Eq. (18) and performing integration over the polar angles, it follows that the TSEP becomes

$$P^s_e = P_0 \sum_{l=1}^{l_{max}} l|\Phi_l(\omega_0/\omega, \phi_z)|^2, \tag{34a}$$

where

$$P_0 = \frac{8\pi}{3}\alpha N \frac{v^2_{max}}{c^2}. \tag{34b}$$

Here, the entire contribution to the TSEP can be seen as the weighted sum over the density of states of the harmonic Fourier components of the velocity squared. Thus, P^s_e in Eq. (34a) is composed of all allowed harmonics permitted by the selection rule of Eq. (16) consistent with the initial condition. Generally, taking into account the symmetry expressed in Eqs. (30a) and (30b), the sum over l in Eq. (34a) can be separated explicitly into the sums over even $(l=2k)$ and odd $(l=2k+1)$ values of l, and written as

$$P^s_e = P_0 \left\{ \sin^2\phi_z \sum_{k=1}^{k_{max}} 2kJ^2_{2k}(\omega_0/\omega) + \cos^2\phi_z \sum_{k=0}^{k_{max}} (2k+1)J^2_{2k+1}(\omega_0/\omega) \right\}, \tag{35}$$

here the phase ϕ_z is defined in Eq. (22b).

It is interesting to note that the TSE probability of Eq. (35) depends explicitly on the phase factor, ϕ_z; this phase factor incorporates into the TSEP an explicit dependence on both the initial electron crystal momentum in the direction of the electric field and the phase of the external ac electric field. This choice of phase dictates the degree of mixing contributions to come from the even and odd harmonic modes reflected in Eqs. (30a) and (30b), respectively. For the initial phase, φ, of the ac field equal to zero, then $\phi_z = aK_{0z}$; thus, when the electrons are initially excited from the bottom of the miniband $(K_{0z}=0)$ or the top of the miniband $(K_{0z} = \pm\frac{\pi}{a})$, then the TSEP will be given by only the superposition of odd harmonic modes. For $K_{0z}=0$ explicitly, the TSEP from Eq. (35) becomes

$$P^s_e = P_0 \sum_{k=0}^{k_{max}} (2k+1)J^2_{2k+1}(\omega_0/\omega). \tag{36}$$

In Figs. 1(a) and 1(b), P^s_e/P_0 from Eq. (36) is graphically represented as a function of ω_0/ω, first in Fig. 1(a) as the first three plateaus in the total sum of Eq. (36), and in Fig. 1(b) as three separate harmonic terms. The TSEP as seen in Fig. 1(a) clearly shows plateaulike step structure with increasing ratio ω_0/ω. The formation of the pronounced plateaus can be understood from Fig. 1(b) by noting the manner in which the contiguous odd harmonic partial sums contribute to the total sum; as the first Bessel-function harmonic

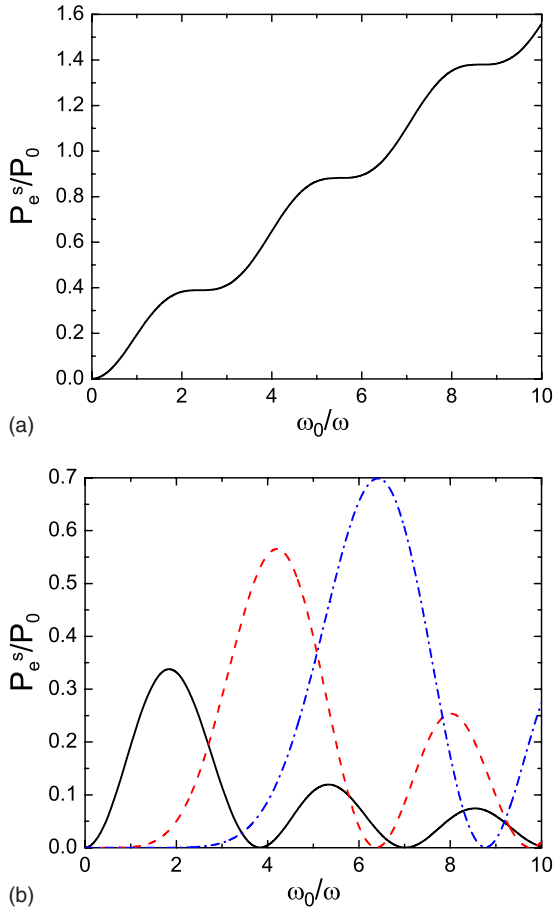

FIG. 1. (Color online) (a) Normalized total SE probability, P_e^s/P_0, defined in Eq. (36) versus ω_0/ω. (b) Normalized partial SE probabilities, $(P_e^s)_m/P_0$, versus ω_0/ω for three odd harmonics $\omega_q = m\omega$ with $m=1$ (solid), $m=3$ (dashed), and $m=5$ (dashed dotted).

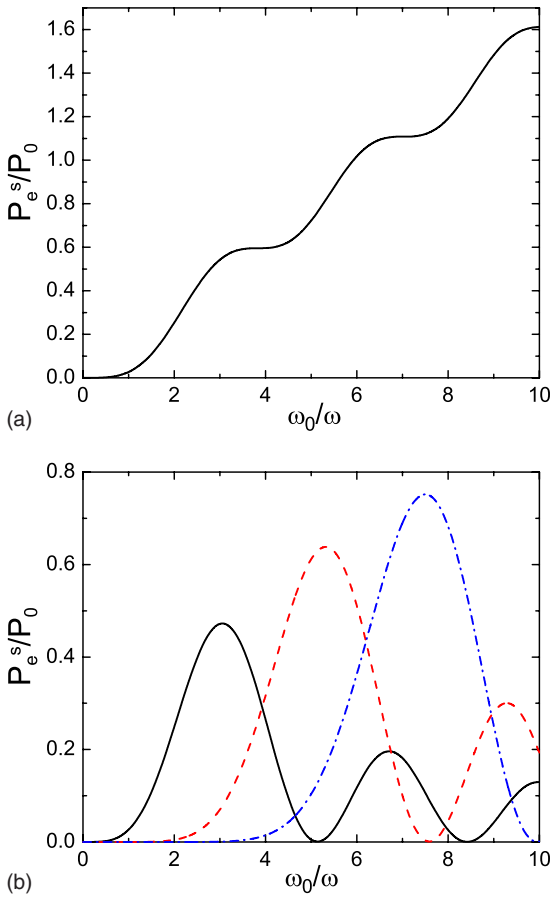

FIG. 2. (Color online) (a) Normalized total SE probability, P_e^s/P_0, defined in Eq. (37) versus ω_0/ω. (b) Normalized partial SE probabilities, $(P_e^s)_m/P_0$, versus ω_0/ω for three even harmonics $\omega_q = m\omega$ with $m=2$ (solid), $m=4$ (dashed), and $m=6$ (dashed dotted).

decreases (solid line) with increasing ω_0/ω, the third Bessel-function harmonic (dashed line) increases and at crossover, perfectly interferes with the decrease in the first harmonic to render a plateau. This crossover interference occurs again in Fig. 1(b) for the decreasing third (dashed line) Bessel-function harmonic and the fifth (dashed-dotted line) Bessel-function harmonic. This type of crossover interference occurs for all the contiguous Bessel-function harmonics and, in principle, renders plateaus to high, physically acceptable values of ω_0/ω. Similarly, for the case when the phase of the ac field is zero, the electron initial condition for K_{0z} could be chosen so that it is excited from the inflection point of the miniband, that is, at $K_{0z} = \pm\frac{1}{2}\frac{\pi}{a}$, and where the velocity is a maximum. Then the TSEP from Eq. (35) becomes

$$P_e^s = P_0 \sum_{k=1}^{k_{max}} 2kJ_{2k}^2(\omega_0/\omega). \tag{37}$$

In Figs. 2(a) and 2(b), P_e^s/P_0 from Eq. (37) is graphically represented as a function of ω_0/ω, as was done in Figs. 1(a) and 1(b) for Eq. (36). A comparison of Figs. 1(a), 1(b), 2(a), and 2(b) shows that the comparative corresponding step positions in Fig. 2(a) are slightly shifted to the right and upward from those in Fig. 1(a) due to the higher-indexed harmonic terms contributing for each corresponding step. Overall, since the ratio of the sums in Eq. (35) is of the order of unity, the TSEP shows a smooth dependence on the initial phase and the step structure as a function of ω_0/ω is preserved for the entire range of phase values $\phi_z \in [0, \pi]$ as demonstrated in Fig. 3. Figure 4 shows the first three bands of the normalized TSEP, $P_e^s/P_0 \simeq$ const, corresponding to three plateaus in Fig. 1(a). For numerical estimations, a GaAs-based SL structure with the SL lattice parameter $a = 75$ Å is assumed. For the SL miniband structure, in the nearest-neighbor tight-binding approximation, it is assumed that the lowest miniband energy width, Δ, is 65 meV so that the maximum group velocity in the miniband is $v_{max} = a\Delta/(2\hbar) = 3.7 \times 10^7$ cm/s. In noting Figs. 1(a) and 1(b), it is observed that $\omega_0/\omega = 1.9$ is the dominant peak contribution for the first harmonic mode and that $\omega_0/\omega = 4.2$ is the dominant peak contribution to the third harmonic mode of the TSEP, with all other contributions to these modes considered negligible when these two specific ratios of ω_0/ω are chosen. Then, for any ratio of ω_0/ω in the range $1.9 < \omega_0/\omega < 4.2$, a mixing of the first and third harmonic modes will take place. If the frequency of the ac field is $f = 1.25$ THz, which corresponds to $\hbar\omega = 5.1$ meV, then $\hbar\omega_0$ for the dominant first harmonic gives $\hbar\omega_0 = 9.7$ meV, which corresponds to an ac-field amplitude of $E_0 = 12.9$ kV/cm; at this ac frequency, the

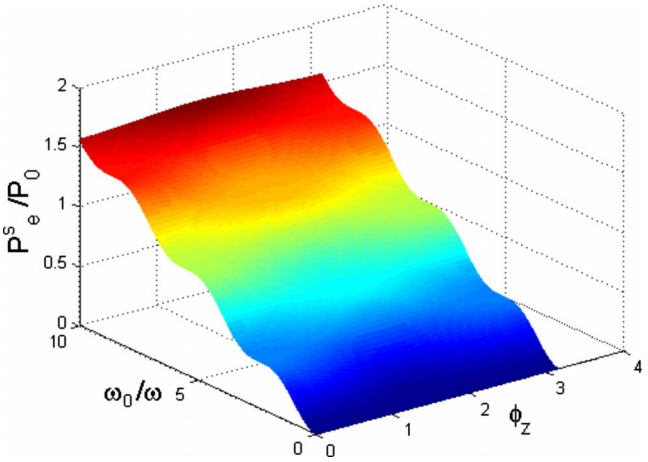

FIG. 3. (Color online) Normalized total SE probability, P_e^s/P_0, versus ω_0/ω defined in Eq. (35) for $0 \le \phi_z \le \pi$.

$\hbar\omega_0$ for the dominant third harmonic corresponds to $\hbar\omega_0 = 21.4$ meV, which corresponds to an ac-field amplitude of $E_0 = 28.5$ kV/cm. Both field-amplitude values are well below the threshold for Zener tunneling in GaAs. It then follows from Eq. (34b) that the SE-probability factor P_0 for $N = 100$ is estimated to be $P_0 = 9.3 \times 10^{-6}$. This value of P_0 leads to similar order-of-magnitude power output as achieved in dc field spontaneous emission due to Bloch oscillations.[13]

Here, for completeness, it is noted that Eqs. (19a) and (19b) are general result for a given electron velocity. In this regard, one can easily see that for a free particle in the ac field of Eq. (3), that $\mathbf{v}(t) = \hbar\mathbf{k}_0(t)/m_0$, where $\mathbf{k}_0(t) = k_{0z}(t) + \mathbf{K}_{0\perp}$; here, $k_{0z}(t)$ is defined in Eq. (8) and $\mathbf{K}_{0\perp}$ is independent of time. Thus Eqs. (19a) and (19b) for the free electron in an ac field become

$$A_{\mathbf{q},j}^{(e)}(\mathbf{k}_0, \tau) = \frac{D\tau}{\sqrt{q}}(\hat{\boldsymbol{\varepsilon}}_{\mathbf{q},j})_z \langle v_z \rangle_{m\omega}, \tag{38a}$$

where

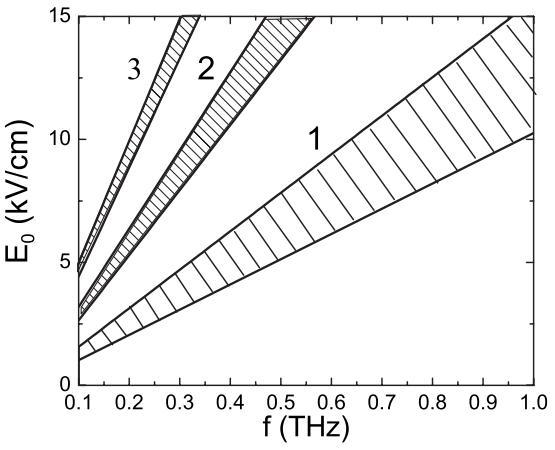

FIG. 4. Three bands (dashed) of constant values of the normalized total SE probability, $P_e^s/P_0 = \text{const}$, shown on the plane (f, E_0) corresponding to three plateaus in Fig. 1(a).

$$\langle v_z \rangle_{m\omega} = i\frac{eE_0}{2m_0\omega} e^{-i\varphi}\delta_{m,1}. \tag{38b}$$

In comparison with the single-band result of Eq. (27), it was found for the nearest-neighbor tight-binding crystal case of Eqs. (30a), (30b), and (31) that

$$\langle v_z \rangle_{m\omega} = i\frac{a\Delta}{2\hbar} e^{-im\varphi}\Phi_m(\omega_0/\omega, \phi_z), \tag{39a}$$

where $\Phi_m(\omega_0/\omega, \phi_z)$ is given in Eq. (30a) for even harmonics ($m = 2k$) and in Eq. (30b) for odd harmonics ($m = 2k+1$). The nearest-neighbor tight-binding results go over to the "free particle in ac field" result in the limit that the lattice parameter, a, vanishes ($a \to 0$), and the band width, Δ, goes to infinity ($\Delta \to \infty$) such that the product $a^2\Delta$ goes over to a finite value, namely, $a^2\Delta \to 2\hbar^2/m_0$; this limit allows for the nearest-neighbor tight-binding energy of Eq. (28) to go over to the free-particle energy dispersion, $\varepsilon(K_z) = \hbar^2 K_z^2/2m_0$, in the K_z direction. In taking this free-particle limit in Eq. (39a), one finds that

$$\langle v_z \rangle_{m\omega} = i\frac{eE_0}{2m_0\omega} e^{-im\varphi}\delta_{m,1}, \tag{39b}$$

which goes over to the free particle in the ac-field result of Eq. (38b). In the final analysis, putting D, defined from Eq. (7), and $\tau = 2\pi/\omega$ into $A_{\mathbf{q}_l,j}^{(e)}$ of Eqs. (38a) and (38b) gives

$$|A_{\mathbf{q}_l,j}^{(e)}(\mathbf{k}_0, \tau)|^2 = 2\pi^3\alpha\frac{e^2E_0^2}{m_0^2\omega^4 q_l V}|(\hat{\boldsymbol{\varepsilon}}_{\mathbf{q}_l,j})_z|^2\delta_{l,1} \tag{40}$$

and putting $|A_{\mathbf{q}_l,j}^{(e)}|^2$ into Eq. (17) while executing the appropriate integration and sum over $l = 1$ only, gives for the *free-particle* total spontaneous-emission probability

$$P_0 = \frac{2\pi}{3}\alpha N\left(\frac{eE_0}{m_0\omega c}\right)^2. \tag{41}$$

This brief comparison shows that for a Bloch electron in an ac field, the Bloch electron accelerates in the band while emitting radiation by spontaneous emission in multiples of the ac-field modes, reflecting the band environment in accordance with the selection rules of Eq. (16); on the other hand, a free electron in an ac field will accelerate in free space while emitting radiation by spontaneous emission *only* at the frequency of the ac field which is essentially the well-known Thompson scattering result.[17]

IV. MICROCAVITY ENHANCEMENT AND TUNING OF SPONTANEOUS EMISSION

In this section, consideration is now focused on the SL structure placed into a rectangular waveguide with cross section $L_x \times L_y$ and length L_z, where the coordinate axis y is chosen along the ac electric field which is also the SL growth direction. The objective here is to enhance and harmonically tune the SE due to the microcavity modal environment.[14] Note that the direction of the ac field has been redirected from the previous discussion in the paper for convenience in considering the specific cavity geometry. For such geometry,

the radiated electromagnetic field inside the waveguide is determined by the guided modes characterized by propagation constant q_z. For purposes of the calculation, consideration is restricted to the dominant TE_{10} mode of a waveguide with $L_x > L_y$; in this case, the vector-potential term in Eq. (5) has only one vector component given by

$$A_{r,y} = \sum_{q_z} \sqrt{\frac{4\pi\hbar c^2}{\omega_q \varepsilon V}} \sin(q_x x)(\hat{a}_q e^{iq_z z} + \hat{a}_q^{\dagger} e^{-iq_z z}), \quad (42)$$

where $\omega_q = \omega_c[1+(q_z/q_x)^2]^{1/2}$ is the modal dispersion relation,[21,22] $\omega_c = q_x c/\sqrt{\varepsilon}$ is the cutoff frequency, $q_x = \pi/L_x$, $V = L_x L_y L_z$, and ε is the dielectric constant of the medium filling the waveguide. It is noted that for the TE_{10} mode, two components of the electric field are equal to zero ($E_x = E_z = 0$) and the mode polarization is along the y axis. Therefore, the polarization index ($j=1$) will be omitted throughout this section. Then, the SE-probability amplitude in the cavity waveguide [compare with Eq. (7)] takes the form

$$A_q(\mathbf{k}_0, t) = D_c (q_x/q)^{1/2} \int_0^t dt' v_y(\mathbf{k}_0 - \mathbf{q}) \times \exp\left\{ -\frac{i}{\hbar} \int_0^{t'} [\varepsilon_{n_0}(\mathbf{k}_0) - \varepsilon_{n_0}(\mathbf{k}_0 - \mathbf{q}) - \hbar\omega_q] dt_1 \right\}, \quad (43)$$

where $D_c = -i\sqrt{\pi c \alpha/\omega_c \varepsilon V}$, $\mathbf{q} = \{\pm q_x, 0, q_z\}$ (with the "+" used for $s=1$ and the "−" used for $s=2$), $q = (q_x^2 + q_z^2)^{1/2}$, and $v_y[\mathbf{k}(t)] = (1/\hbar)\nabla_{\mathbf{K}_y} \varepsilon(\mathbf{K})|_{\mathbf{k}(t)}$, the y component of Bloch velocity in the band. Also, the probability amplitude, $A_{\mathbf{q}}^{(e)}(\mathbf{k}_0, \tau)$, over a single ac-field period τ is

$$A_q(\mathbf{k}_0, \tau) = D_c (q_x/q)^{1/2} \int_0^{\tau} dt v_y(\mathbf{k}_0 - \mathbf{q}) \times \exp\left\{ -\frac{i}{\hbar} \int_0^{t} [\varepsilon_{n_0}(\mathbf{k}_0) - \varepsilon_{n_0}(\mathbf{k}_0 - \mathbf{q}) - \hbar\omega_q] dt_1 \right\}. \quad (44)$$

From the condition for maximum growth of the probability amplitude, at integral multiples of the ac-field period, the selection rule for the photon-emission frequency in the presence of a resonant cavity is established in a similar fashion to Eq. (16) as

$$\omega_q = m\omega, \quad q_z = \pm q_{zm}, \quad (45)$$

where $q_{zm} = q_x[(m\omega/\omega_c)^2 - 1]^{1/2}$. This probability amplitude is now used for the calculation of the TSEP with $t = N\tau$ to obtain

$$P_e^s = N \frac{L_z \omega}{L_x \omega_c} \sum_{l=1}^{l_{max}} \sum_{s=1,2} \frac{|A_{\mathbf{q}_l}^{(e)}(\mathbf{k}_0, \tau)|^2}{\sqrt{1-(q_x/q_l)^2}}. \quad (46)$$

In keeping the terms to zeroth order in $\mathbf{q}$ only, the probability amplitude in Eq. (44), instead of Eqs. (19a) and (19b), becomes

$$A_{\mathbf{q}}^{(e)}(\mathbf{k}_0, \tau) = i \frac{D_c a}{\hbar} \left(\frac{q_x}{q}\right)^{1/2} \int_0^{\tau} dt' \sum_{\ell} \ell_y \epsilon(\ell) e^{i[\ell \cdot \mathbf{k}_0(t') + \omega_q t']}. \quad (47)$$

Following some straightforward calculations, as performed in Eqs. (19a) and (19b), Eq. (47) becomes

$$A_{\mathbf{q}_m}^{(e)}(\mathbf{k}_0, \tau) = \frac{2\pi i D_c}{\hbar\omega} \left(\frac{q_x}{q}\right)^{1/2} \sum_{\ell_y} \epsilon(a\ell_y, \mathbf{K}_{0\perp}) \times a\ell_y e^{i\ell_y \phi_y} J_m\left(\ell_y \frac{\omega_0}{\omega}\right) e^{im\varphi}, \quad (48)$$

where $\phi_y = aK_{0y} - \frac{\omega_0}{\omega}\sin\varphi$. For the nearest-neighbor tight-binding energy-band approximation, the probability amplitude in Eq. (48) is simplified to become

$$A_{\mathbf{q}_m}^{(e)}(\mathbf{k}_0, \tau) = -\frac{2\pi i D_c}{\omega} \left(\frac{q_x}{q}\right)^{1/2} v_{max} e^{im\varphi} \Phi_m(\omega_0/\omega, \phi_y), \quad (49)$$

where $\Phi_m(\omega_0/\omega, \phi_y)$ is given by Eq. (30a) for even ($m = 2k$) harmonics and is given by Eq. (30b) for odd ($m = 2k+1$) harmonics. Then, the squared probability amplitude becomes

$$|A_{\mathbf{q}_l}^{(e)}(\mathbf{k}_0, \tau)|^2 = 4\pi^3 \alpha \frac{v_{max}^2}{\omega^2 q_l \varepsilon^{1/2} V} |\Phi_l(\omega_0/\omega, \phi_y)|^2 \quad (50)$$

and the TSEP in Eq. (46) results in

$$P_e^s = P_{0c} \frac{\omega_c^2}{\omega^2} \sum_{l=1}^{l_{max}} \frac{1}{l} \frac{1}{\sqrt{1-(\omega_c/l\omega)^2}} |\Phi_l(\omega_0/\omega, \phi_y)|^2, \quad (51a)$$

where

$$P_{0c} = 4\alpha N \varepsilon^{1/2} \frac{L_x}{L_y} \frac{v_{max}^2}{c^2}. \quad (51b)$$

As noted in the free-space case of Eq. (34a), the TSEP in Eq. (51a) can be seen as a weighted sum over the cavity density of states of the harmonic Fourier components of the velocity squared. Specifically, the microcavity TSEP given for the superposition of odd harmonic modes from Eq. (51a), as compared to the free-space TSEP result of Eq. (36), becomes

$$P_e^s = P_{0c} \frac{\omega_c^2}{\omega^2} \sum_{k=0}^{k_{max}} \frac{1}{2k+1} \frac{1}{\sqrt{1-\left[\frac{\omega_c}{(2k+1)\omega}\right]^2}} J_{2k+1}^2(\omega_0/\omega). \quad (52)$$

The normalized microcavity TSEP, P_e^s/P_{0c}, of Eq. (52) is shown in Fig. 5 as a function of the ratio ω_0/ω for two different *tuning* values of the ac-field frequency, ω, relative to the waveguide cutoff frequency, ω_c. For the relative choice of cutoff frequency given by the ratio $\omega/\omega_c = 1.1$, the solid curve of Fig. 5 shows the behavior of P_e^s/P_{0c}; this choice of $\omega/\omega_c = 1.1$ has essentially selected from the harmonic sum of Eq. (52) the first basic harmonic corresponding to $k=0$ or correspondingly $m=1$ of the selection

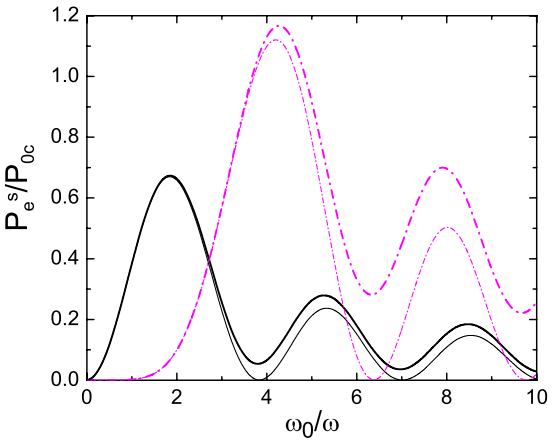

FIG. 5. (Color online) Normalized total SE probability, P_e^s/P_{0c}, [Eq. (52)] versus ω_0/ω for different tuning of ω to the waveguide cutoff frequency, ω_c, to select the basic harmonic $\omega/\omega_c=1.1$ (thick solid) and the third harmonic (3ω) $3\omega/\omega_c=1.1$ (thick dashed dotted). The thin curves correspond to the first (solid) and third (dashed-dotted) harmonics alone, respectively.

rule from Eq. (45). For the first basic harmonic, the enhancement factor $\eta=(P_e^s)_{cav}/(P_e^s)_{fs}$, i.e., the ratio between the cavity and free-space TSEP, is given by $\eta=3L_x\varepsilon^{1/2}/2\pi L_y(\omega/\omega_c)\sqrt{(\omega/\omega_c)^2-1}$, which is a function of the normalized frequency ω/ω_c and increases monotonically with decreasing ratio ω/ω_c. Taking for an estimation $\omega/\omega_c=1.1$, $L_x/L_y=2$, and $\varepsilon=12.2$, one obtains $\eta=6.7$ which suggests that when the frequency ω is tuned close to the cavity cutoff frequency, the SE enhancement value will be increased approximately 1 order of magnitude over unity. It is clear that this result differs from the free-space result of Eq. (37) in two significant ways; the coefficient of harmonic $J_l^2(\omega_0/\omega)$ in Eq. (52) is different by the prefactor $\frac{1}{l}\frac{1}{\sqrt{1-(\omega_c/l\omega)^2}}$ arising from the cavity tuning; second, the harmonic has been isolated from adjacent modes by tuning to the cavity cutoff frequency, thus removing the plateau originally observed in Fig. 1(a). Also from Fig. 5, for the relative choice of $\omega/\omega_c=0.37$, which gives rise to cutoff frequency condition at 3ω since $3\omega/\omega_c=1.1$, then the third harmonic $J_3^2(\omega_0/\omega)$ in the dash-dotted curve is dominant and is enhanced by the prefactor of Eq. (52) while the basic harmonic $J_1^2(\omega_0/\omega)$ is filtered out by the cutoff condition. Thus the influence of the cavity is to *enhance* and *selectively tune* to the desired harmonics of the TSEP spectrum.

V. TOTAL SPONTANEOUS-EMISSION PROBABILITY: TEMPERATURE- AND DENSITY-DEPENDENT ANALYSIS IN THE INDEPENDENT ELECTRON APPROXIMATION

The temperature-independent one-electron total SE probability is given, at any time, t, in Eq. (6) as

$$P_e^s(t)=\sum_{\mathbf{q},j}|A_{\mathbf{q},j}^{(e)}(\mathbf{k}_0,t)|^2, \tag{53}$$

where $\mathbf{k}_0(t)=\mathbf{K}_0+\mathbf{p}_c(t)/\hbar$ is the time-dependent wave vector associated with the instantaneous energy eigenstates of H_0, and $\mathbf{K}_0$ is the initial value of the wave vector $\mathbf{k}_0(t)$. At time $t=N\tau$, where $\tau=2\pi/\omega$, the ac-field period and N is a positive integer, it was determined that P_e^s in Eq. (53) reduced to a simple function of the initial wave vector, K_{0z}, in the $\hat{z}$ direction alone; this determination is explicitly noted in Eq. (35) for the TSE into free space, and in Eq. (51a) for the TSE into a microcavity mode.

In order to extend the one-electron TSE probability of Eq. (53) so as to properly describe the situation for a system of electrons at constant density, n, and at a thermal equilibrium temperature, T, based on the independent electron approximation, use is made of the density matrix for the electron-photon system to describe the TSE probability to first order in the radiation field. In this regard, the density-matrix method proceeds in a manner similar to that described in the previous work developed by two of the present authors (Krieger and Iafrate);[15,16] here, as an extension, the density-matrix development is presented for an interacting electron-photon system.

We start with the Liouville equation for the density matrix ϱ as

$$i\hbar\frac{\partial\varrho}{\partial t}=[H,\varrho], \tag{54}$$

where H has been specified below Eq. (4) as

$$H=H_0+H_r+H_I. \tag{55}$$

Here, H_0 is given by

$$H_0(t)=[\mathbf{p}+\mathbf{p}_c(t)]^2/2m_0+V_c(\mathbf{r}), \tag{56}$$

the Hamiltonian for a single electron in a periodic crystal potential, $V_c(\mathbf{r})$, interacting with a homogeneous ac electric field, $\mathbf{p}_c(t)$, specified by Eqs. (3) and (4); H_r is given by

$$H_r=\sum_{\mathbf{q},j}\hbar\omega_q a_{\mathbf{q},j}^\dagger a_{\mathbf{q},j}, \tag{57}$$

the Hamiltonian for the free-quantized radiation field; and H_I is given by

$$H_I(t)=-\frac{e}{m_0c}[\mathbf{p}+\mathbf{p}_c(t)]\cdot\mathbf{A}_r, \tag{58}$$

where

$$\mathbf{A}_r=\sqrt{\frac{2\pi\hbar c}{V}}\sum_{\mathbf{q},j}\frac{\hat{\boldsymbol{\varepsilon}}_{\mathbf{q},j}}{\sqrt{q}}(a_{\mathbf{q},j}e^{i\mathbf{q}\cdot\mathbf{r}}+a_{\mathbf{q},j}^\dagger e^{-i\mathbf{q}\cdot\mathbf{r}}), \tag{59}$$

the first-order interaction between H_0 and H_r to achieve SE transitions.

The basis states that are utilized in evaluating the matrix elements of the density operator in Eq. (54) are the instantaneous eigenstates of H_0 in Eq. (56) and the eigenstates of H_r in Eq. (57). These eigenstates satisfy

$$H_0(t)\psi_{\mathbf{k}(t)}=\varepsilon[\mathbf{k}(t)]\psi_{\mathbf{k}(t)}, \tag{60}$$

where

$$\psi_{\mathbf{k}(t)}(\mathbf{r},t) = \frac{e^{i\mathbf{K}\cdot\mathbf{r}}}{V^{1/2}} u_{\mathbf{k}(t)}(\mathbf{r}); \tag{61}$$

here, $u_{\mathbf{k}(t)}(\mathbf{r})$ is the periodic part of the Bloch function, $\mathbf{k}(t) = \mathbf{K} + \mathbf{p}_c(t)/\hbar$, where the values of $\mathbf{K}$ are determined by the periodic boundary conditions of the periodic crystal of volume V. As well,

$$H_r|\{n_{\mathbf{q},j}\}\rangle = \sum_{\mathbf{q},j} \hbar\omega_q n_{\mathbf{q},j}|n_{\mathbf{q},j}\rangle, \tag{62}$$

where $|\{n_{\mathbf{q},j}\}\rangle$ is a simple product of all possible combinations of photon number states, $n_{\mathbf{q},j}$, with a given wave vector $\mathbf{q}$ and polarization $\hat{\varepsilon}_{\mathbf{q},j}$.

In this calculation, we are specifically concerned with *one-photon* spontaneous emission. Therefore, we consider only matrix elements connecting quantum field states $|0,0,0,\ldots,0,0\rangle \equiv |0\rangle$, the vacuum state, and $|0,\ldots,1_j,0\ldots\rangle \equiv |1_j\rangle$, the one-photon excited state j with wave vector $\mathbf{q}$ and polarization $\hat{\varepsilon}_{\mathbf{q},j}$. Then the matrix element of H_I in Eq. (58) with respect to $|1_j\rangle$ and $|0\rangle$ becomes

$$\langle 1_j|H_I|0\rangle = -\frac{e}{m_0 c}(\mathbf{p}+\mathbf{p}_c)\langle 1_j|\mathbf{A}_r|0\rangle = -\frac{\hbar}{m_0}\sqrt{\frac{2\pi\alpha}{Vq}}(\mathbf{p}+\mathbf{p}_c)\cdot\hat{\varepsilon}_{\mathbf{q},j}e^{-i\mathbf{q}\cdot\mathbf{r}}. \tag{63}$$

In further taking the matrix element of H_I in Eq. (63) with respect to instantaneous eigenstates $\psi_{\mathbf{k}(t)}(\mathbf{r},t) \equiv |\mathbf{k}(t)\rangle$, we obtain

$$\langle \mathbf{k},1_j|H_I|\mathbf{k}',0\rangle = -\frac{\hbar}{m_0}\sqrt{\frac{2\pi\alpha}{Vq}}\hat{\varepsilon}_{\mathbf{q},j}\cdot\langle\mathbf{k}|(\mathbf{p}+\mathbf{p}_c)e^{-i\mathbf{q}\cdot\mathbf{r}}|\mathbf{k}'\rangle, \tag{64}$$

where $|\mathbf{k},1_j\rangle = |\mathbf{k}\rangle|1_j\rangle$ and $|\mathbf{k}',0\rangle = |\mathbf{k}'\rangle|0\rangle$. The integral over instantaneous eigenstates has been evaluated previously[13] for $qa \ll 1$ and is expressed as

$$\langle\mathbf{k}|(\mathbf{p}+\mathbf{p}_c)e^{-i\mathbf{q}\cdot\mathbf{r}}|\mathbf{k}'\rangle = m_0\mathbf{v}(\mathbf{k})\delta_{\mathbf{k}',\mathbf{k}+\mathbf{q}}, \tag{65}$$

where $\mathbf{v}(\mathbf{k})$ is the Bloch velocity. Thus, the matrix element of H_I in Eq. (64) is explicitly expressed as

$$\langle \mathbf{k},1_j|H_I|\mathbf{k}',0\rangle = -\hbar\sqrt{\frac{2\pi\alpha}{Vq}}\hat{\varepsilon}_{\mathbf{q},j}\cdot\mathbf{v}(\mathbf{k})\delta_{\mathbf{k}',\mathbf{k}+\mathbf{q}}. \tag{66}$$

It then follows from first-order time-dependent perturbation theory that the SE amplitude for a transition from state $|\mathbf{k}',0\rangle$ to $|\mathbf{k},1_j\rangle$ is given by

$$A^{(1)}(\mathbf{k}',\mathbf{k}) = \int_{t_0}^{t} dt'\langle\mathbf{k},1_j|\frac{1}{i\hbar}H_I(t')|\mathbf{k}',0\rangle \times\exp\left\{-\frac{i}{\hbar}\int_{t_0}^{t'}[\varepsilon(\mathbf{k}')-\varepsilon(\mathbf{k})-\hbar\omega_q]dt_1\right\}. \tag{67}$$

Using matrix elements of Eq. (66) in Eq. (67), the SE transition amplitude reduces to

$$A^{(1)}(\mathbf{k}',\mathbf{k}=\mathbf{k}'-\mathbf{q}) = \frac{D}{\sqrt{q}}\int_{t_0}^{t} dt'\mathbf{v}(\mathbf{k}'-\mathbf{q})\cdot\hat{\boldsymbol{\varepsilon}}_{\mathbf{q},j}\exp\left\{-\frac{i}{\hbar}\int_{t_0}^{t'}\{\varepsilon(\mathbf{k}') - \varepsilon(\mathbf{k}'-\mathbf{q})-\hbar\omega_q\}dt_1\right\}, \tag{68}$$

where $D = -i\sqrt{2\pi\alpha/V}$. Thus Eq. (68) is the SE amplitude for a transition from electronic state $\mathbf{k}' = \mathbf{K}' + \mathbf{p}_c/\hbar$, with no photons in the quantum radiation field, to the electronic state $\mathbf{k}'-\mathbf{q}$, with one photon of wave vector $\mathbf{q}$ and photon energy, $\hbar\omega_q = m\hbar\omega$ [see Eq. (16)], in the quantum radiation field. The result in Eq. (68) is the same as the result reported in Eq. (7) with $A^{(1)}$ given by $A^{(e)}_{\mathbf{q},j}(\mathbf{k}_0,t)$ and $\mathbf{k}'(t) \equiv \mathbf{k}_0(t) = \mathbf{K}_0 + \mathbf{p}_c(t)/\hbar$.

In considering the matrix elements of the density matrix in Eq. (54) with the Hamiltonian of Eqs. (55)–(59), and using the basis states from Eqs. (60)–(62) with special interest in the diagonal density-matrix connection between states $|\mathbf{k}',0\rangle$ and $|\mathbf{k},1_j\rangle$, it is noted for general photon index "n," and $\varrho_{\mathbf{k}'n'\mathbf{k}n} \equiv \langle\mathbf{k}'n'|\varrho|\mathbf{k}n\rangle$, that

$$i\hbar\frac{\partial\varrho_{\mathbf{k}'n'\mathbf{k}n}}{\partial t} = [H,\varrho]_{\mathbf{k}'n'\mathbf{k}n} = [\varepsilon(\mathbf{k}')-\varepsilon(\mathbf{k})]\varrho_{\mathbf{k}'n'\mathbf{k}n} + \hbar\omega_q(n'-n)\varrho_{\mathbf{k}'n'\mathbf{k}n} + \sum_{\mathbf{k}''n''}[(H_I)_{\mathbf{k}'n'\mathbf{k}''n''}\varrho_{\mathbf{k}''n''\mathbf{k}n} - \varrho_{\mathbf{k}'n'\mathbf{k}''n''}(H_I)_{\mathbf{k}''n''\mathbf{k}n}]. \tag{69}$$

Here, a single-band analysis is assumed and, therefore, Zener-band tunneling is ignored through the assumption that $(\frac{\partial\varrho}{\partial t})_{\mathbf{k}'n'\mathbf{k}n} \equiv \frac{\partial}{\partial t}\varrho_{\mathbf{k}'n'\mathbf{k}n}$. From Eq. (69), it follows that the equation for the diagonal matrix elements $[(\mathbf{k}'n') = (\mathbf{k}n)]$ becomes

$$i\hbar\frac{\partial\varrho_{\mathbf{k}n\mathbf{k}n}}{\partial t} = \sum_{\mathbf{k}''n''\neq\mathbf{k}n}[(H_I)_{\mathbf{k}n\mathbf{k}''n''}\varrho_{\mathbf{k}''n''\mathbf{k}n} - \{(H_I)_{\mathbf{k}n\mathbf{k}''n''}\varrho_{\mathbf{k}''n''\mathbf{k}n}\}^*]. \tag{70}$$

For the diagonal and off-diagonal matrix elements, which appear on the right-hand side of Eq. (69), we obtain

$$i\hbar\frac{\partial\varrho_{\mathbf{k}'n'\mathbf{k}n}}{\partial t} = [\varepsilon(\mathbf{k}')-\varepsilon(\mathbf{k})+\hbar\omega_q(n'-n)]\varrho_{\mathbf{k}'n'\mathbf{k}n} + (H_I)_{\mathbf{k}'n'\mathbf{k}n}(\varrho_{\mathbf{k}n\mathbf{k}n}-\varrho_{\mathbf{k}'n'\mathbf{k}'n'}) + \sum_{\mathbf{k}''n''\neq\mathbf{k}'n',\mathbf{k}n}[(H_I)_{\mathbf{k}'n'\mathbf{k}''n''}\varrho_{\mathbf{k}''n''\mathbf{k}n} - \varrho_{\mathbf{k}'n'\mathbf{k}''n''}(H_I)_{\mathbf{k}''n''\mathbf{k}n}]. \tag{71}$$

Since we are looking for the lowest-order approximation in $(H_I)_{\mathbf{k}'n'\mathbf{k}''n''}$, off-diagonal density-matrix elements beyond the states connecting $(\mathbf{k}'n')$ and $(\mathbf{k}n)$ are neglected in the sum on the right-hand side of Eq. (71). Thus, the off-diagonal matrix elements are connected to the diagonal elements through lowest order in H_I as

$$i\hbar\frac{\partial \varrho_{\mathbf{k}'n'\mathbf{k}n}}{\partial t} = [\varepsilon(\mathbf{k}') - \varepsilon(\mathbf{k}) + \hbar\omega_q(n'-n)]\varrho_{\mathbf{k}'n'\mathbf{k}n} + (H_I)_{\mathbf{k}'n'\mathbf{k}n}(\varrho_{\mathbf{k}n\mathbf{k}n} - \varrho_{\mathbf{k}'n'\mathbf{k}'n'}). \quad (72)$$

Thus, in fixing the initial condition on the off-diagonal elements, $\varrho_{\mathbf{k}'n'\mathbf{k}n}(t_0)=0$ in Eq. (72), we can formally integrate Eq. (72) for $\varrho_{\mathbf{k}'n'\mathbf{k}n}(t)$ and insert the result into Eq. (70) to obtain a closed expression for the diagonal density-matrix elements valid to second order in H_I. Letting $\varrho_{\mathbf{k}n\mathbf{k}n} \equiv \varrho_{\mathbf{k}n}$, we obtain

$$\frac{\partial \varrho_{\mathbf{k}n}}{\partial t} = \sum_{\mathbf{k}''n''\neq\mathbf{k}n} \left\{ \left[\frac{1}{i\hbar}H_I(t)\right]_{\mathbf{k}n\mathbf{k}''n''} \times \exp\left\{-\frac{i}{\hbar}\int_{t_0}^{t} dt_1[\varepsilon(\mathbf{k}'') - \varepsilon(\mathbf{k}) + \hbar\omega_q(n''-n)]\right\} \times \int_{t_0}^{t} dt' \left[\frac{1}{i\hbar}H_I(t')\right]_{\mathbf{k}''n''\mathbf{k}n} [\varrho_{\mathbf{k}n}(t') - \varrho_{\mathbf{k}''n''}(t')] \times \exp\left\{\frac{i}{\hbar}\int_{t_0}^{t'} dt_1[\varepsilon(\mathbf{k}'') - \varepsilon(\mathbf{k}) + \hbar\omega_q(n''-n)]\right\} + \text{c.c.}\right\}, \quad (73)$$

a closed equation for the diagonal matrix elements, $\varrho_{\mathbf{k}n}$, accurate to second order in the interaction Hamiltonian, H_I.

In connecting the interaction between *single*-photon states $|0\rangle$ and $|1_j\rangle$ only in Eq. (73), we let $n \rightarrow$ "1_j" and $n'' \rightarrow$ "0", and use Eqs. (66) and (67) in Eq. (73) to obtain

$$\frac{\partial \varrho_{\mathbf{k},1}}{\partial t} = \frac{\partial A^{(1)}(\mathbf{k}+\mathbf{q},\mathbf{k},t)}{\partial t}\int_{t_0}^{t} dt' \frac{\partial A^{(1)*}(\mathbf{k}+\mathbf{q},\mathbf{k},t')}{\partial t'} \times [\varrho_{\mathbf{k}+\mathbf{q},0}(t') - \varrho_{\mathbf{k},1}(t')] + \text{c.c.} \quad (74)$$

In letting $\mathbf{k}\rightarrow\mathbf{k}-\mathbf{q}$ and noting that $A^{(1)}(\mathbf{k},\mathbf{k}-\mathbf{q},t) = A^{(e)}_{\mathbf{q},j}(\mathbf{k},t)$, the SE amplitude as defined in Eqs. (7) and (68), we find that Eq. (74) becomes

$$\frac{\partial \varrho_{\mathbf{k}-\mathbf{q},1}}{\partial t} = \frac{\partial A^{(e)}_{\mathbf{q},j}(\mathbf{k},t)}{\partial t}\int_{t_0}^{t} dt' \frac{\partial A^{(e)*}_{\mathbf{q},j}(\mathbf{k},t')}{\partial t'} \times [\varrho_{\mathbf{k},0}(t') - \varrho_{\mathbf{k}-\mathbf{q},1}(t')] + \text{c.c.} \quad (75)$$

Here, we now replace the diagonal density-matrix element, $\varrho_{\mathbf{k},0}(t')$, under the integral of Eq. (75) by the density matrix representing the initial electron-photon conditions. Thus, we let $\varrho_{\mathbf{k},0}(t') \simeq \mathcal{F}_F[\varepsilon(\mathbf{k}_0)]\langle 0|0\rangle$, where $\mathcal{F}_F[\varepsilon(\mathbf{k}_0)]$ is assumed to be the thermal-equilibrium Fermi-Dirac distribution function for the *initial electronic states*, and $\langle 0|0\rangle$ is the initial photon vacuum field normalization assumed to be unity. Then Eq. (75) becomes

$$\frac{\partial \varrho_{\mathbf{k}-\mathbf{q},1}}{\partial t} = \varrho_{\mathbf{k},0}(t_0)\frac{\partial |A^{(e)}_{\mathbf{q},j}(\mathbf{k},t)|^2}{\partial t} - \int_{t_0}^{t} dt' K(t,t')\varrho_{\mathbf{k}-\mathbf{q},1}(t'), \quad (76)$$

where the kernel function $K(t,t')$ is given by

$$K(t,t') = \frac{\partial A^{(e)}_{\mathbf{q},j}(\mathbf{k},t)}{\partial t}\frac{\partial A^{(e)*}_{\mathbf{q},j}(\mathbf{k},t')}{\partial t'} + \frac{\partial A^{(e)*}_{\mathbf{q},j}(\mathbf{k},t)}{\partial t}\frac{\partial A^{(e)}_{\mathbf{q},j}(\mathbf{k},t')}{\partial t'}. \quad (77)$$

For the *final electronic state*, $\varrho_{\mathbf{k}-\mathbf{q},1}(t')$, we perform the integral over $K(t,t')$ in Eq. (76) by parts and retain the lowest-order coherent term in the perturbation (H_I) to obtain

$$\frac{\partial \varrho_{\mathbf{k}-\mathbf{q},1}}{\partial t} = [\varrho_{\mathbf{k},0}(t_0) - \varrho_{\mathbf{k}-\mathbf{q},1}(t)]\frac{\partial |A^{(e)}_{\mathbf{q},j}(\mathbf{k},t)|^2}{\partial t}. \quad (78)$$

This equation can be integrated from t_0 to t and, after using the initial condition $\varrho_{\mathbf{k}-\mathbf{q},1}(t_0)=0$, we obtain

$$\varrho_{\mathbf{k}-\mathbf{q},1}(t) = \varrho_{\mathbf{k},0}(t_0)[1 - \exp(|A^{(e)}_{\mathbf{q},j}(\mathbf{k},t)|^2)]. \quad (79)$$

In the spirit of perturbation theory, with $|A^{(e)}_{\mathbf{q},j}(\mathbf{k},t)|^2 \ll 1$, $\varrho_{\mathbf{k}-\mathbf{q},1}(t)$ can be written to lowest order in $|A^{(e)}_{\mathbf{q},j}(\mathbf{k},t)|^2$, as

$$\varrho_{\mathbf{k}-\mathbf{q},1}(t) = \varrho_{\mathbf{k},0}(t_0)|A^{(e)}_{\mathbf{q},j}(\mathbf{k},t)|^2. \quad (80)$$

Thus, it follows from Eq. (80) that the TSE probability, consistent with a constant temperature and electron density, is given by

$$P^s_e(t) = \sum_{\mathbf{k}_0}\sum_{\mathbf{q},j} \varrho_{\mathbf{k}_0-\mathbf{q},1}(t) = \sum_{\mathbf{k}_0}\sum_{\mathbf{q},j} |A^{(e)}_{\mathbf{q},j}(\mathbf{k}_0,t)|^2 \mathcal{F}_F[\varepsilon(\mathbf{k}_0)]. \quad (81)$$

This expression for $P^s_e(t)$, along with the electron density given by

$$n = \sum_{\mathbf{K}_0} \mathcal{F}_F[\varepsilon(\mathbf{K}_0)] \quad (82)$$

is an extension of Eq. (53) to include temperature and electron-density dependence in the TSE analysis. Here $\mathcal{F}_F[\varepsilon(\mathbf{K}_0)] = 1/(1+e^{[\varepsilon(\mathbf{K}_0)-\varepsilon_F]/K_BT})$ is the Fermi distribution function and ε_F is the Fermi energy. In particular, it is clear from Eq. (81) that the temperature-dependent TSE distributes the given number of electrons over the initial $\mathbf{k}_0$ states of the SL in accordance with the *Fermi distribution* subject to the particle conservation law of Eq. (82) which allows for the determination of the temperature-dependent Fermi energy. At time $t=N\tau$, where τ is the ac-field period and N is a positive integer, it was determined that P^s_e in Eq. (53) reduced to a basic function of the initial wave vector, K_{0z}, in the $\hat{z}$ direction alone; this determination is explicitly noted in Eq. (35) for the TSE into free space, and in Eq. (51a) for the TSE into a microcavity mode. Thus, it follows that the TSE probability can be written as

$$P^s_e = \sum_{\mathbf{K}_0} P^s_e(K_{0z})\mathcal{F}_F[\varepsilon(\mathbf{K}_0),T]. \quad (83)$$

For the energy dispersion associated with the SL model discussed in Eq. (28) while taking for the specific form of $\varepsilon_\perp(\mathbf{K}_\perp)$, namely, $\varepsilon_\perp(\mathbf{K}_\perp) = \hbar^2K^2_\perp/2m^*_\perp$, we then consider $\varepsilon(\mathbf{K})$ to be

$$\varepsilon(\mathbf{K}) = \varepsilon(0) + \Delta \sin^2\frac{aK_z}{2} + \frac{\hbar^2 K_\perp^2}{2m_\perp^*}. \tag{84}$$

Then, in using $\Sigma_{\mathbf{K}}=[2V/(2\pi)^3]\int d\mathbf{K}$, where the factor of 2 indicates electron-spin degeneracy, the sums of Eqs. (82) and (83) can be converted to integrals over $\mathbf{K}$ as

$$n = \frac{2}{(2\pi)^3}\int dK_z \int d\mathbf{K}_\perp \mathcal{F}_F[\varepsilon(K_z,\mathbf{K}_\perp;T)], \tag{85}$$

$$P_e^s = \frac{2}{(2\pi)^3}\int dK_z \int d\mathbf{K}_\perp P_e^s(K_z)\mathcal{F}_F[\varepsilon(K_z,\mathbf{K}_\perp;T)]. \tag{86}$$

Here $\mathbf{K}_\perp$ is taken over polar coordinates $(K_\perp,\theta)$ with $0\le\theta\le 2\pi$ and $0\le K_\perp\le K_{\perp 0}$; K_z is taken over the range $K_z^-\le K_z\le K_z^+$, where the $K_z^\pm$ values are determined from the zeros of $\varepsilon(K_z)-\varepsilon_F=0$, with $\varepsilon(K_z)$ defined from part of $\varepsilon(\mathbf{K})$ in Eq. (84) noted as $\varepsilon(K_z)=\varepsilon(0)+\Delta\sin^2(aK_z/2)$.

In the special case of the zero-temperature limit, that is, $T\to 0$, it is well known that $\mathcal{F}_F$ behaves like a Heaviside function with respect to the Fermi energy. In this case, it is easy to establish that $\varepsilon(K_z)-\varepsilon_F=0$ gives

$$K_z^\pm = \pm\frac{1}{a}\arccos\left[1+\frac{2[\varepsilon(0)-\varepsilon_F]}{\Delta}\right], \tag{87}$$

where ε_F is independent of temperature. One can see that when $\varepsilon_F=\varepsilon(0)$, at the SL band edge, then $K_z^\pm=0$; also, at $\varepsilon_F=\varepsilon(0)+\Delta/2$, at the SL midband, then $K_z^\pm=\pm\pi/2a$; as well, at $\varepsilon_F=\varepsilon(0)+\Delta$, at the SL-band boundaries, then $K_z^\pm=\pm\pi/a$. Thus, for a value of ε_F between $\varepsilon(0)\le\varepsilon_F\le\varepsilon(0)+\Delta$, it is clear that the SL becomes fractionally filled from the band minimum up to the full bandwidth, Δ. The electron density associated with a corresponding Fermi energy is found by evaluating Eq. (85) at $T=0$, and the TSEP at $T=0$, for this density, is found by evaluating Eq. (86). For the special case where the ac-field phase is zero so that $\phi_z=aK_{0z}$, then P_e^s of Eq. (35) can be directly inserted into Eq. (86) where the integrals over $\sin^2(K_{0z}a)$ and $\cos^2(K_{0z}a)$ can be easily evaluated, along with the electron-density expression of Eq. (85), to obtain

$$\frac{P_e^s}{n^* P_0} = A_1(\varepsilon_F)\sum_{k=0}^{k_{max}}(2k+1)J_{2k+1}^2(\omega_0/\omega) + A_2(\varepsilon_F)\sum_{k=1}^{k_{max}}2kJ_{2k}^2(\omega_0/\omega) \tag{88}$$

and

$$\frac{n}{n^*} = (1-\gamma^2)^{1/2} - \gamma\arccos(\gamma). \tag{89}$$

Here

$$A_1(\varepsilon_F) = \frac{1}{2}\left[\frac{n}{n^*}+\frac{1}{3}(1-\gamma^2)^{3/2}\right],$$

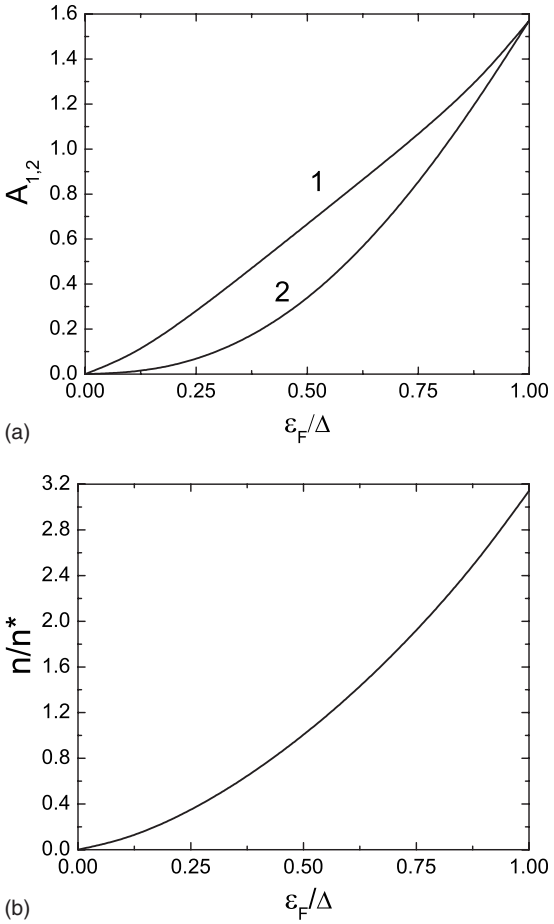

FIG. 6. (a) The coefficients A_1 (curve 1) and A_2 (curve 2) [Eq. (90)], and (b) normalized electron density n/n^* [Eq. (89)] as functions of the ratio ε_F/Δ.

$$A_2(\varepsilon_F) = \frac{1}{2}\left[\frac{n}{n^*}-\frac{1}{3}(1-\gamma^2)^{3/2}\right], \tag{90}$$

where $n^*=m_\perp^*\Delta/(2\pi^2\hbar^2a^2)$ and $\gamma=1+2[\varepsilon(0)-\varepsilon_F]/\Delta$ with $-1\le\gamma\le 1$; putting $\gamma=\gamma(\varepsilon_F)$ into Eqs. (89) and (90) makes n/n^* and A_1,A_2 explicit functions of $\frac{\varepsilon_F}{\Delta}=\frac{\varepsilon(0)}{\Delta}+\frac{1}{2}(1-\gamma)$ as noted in Figs. 6(a) and 6(b) with $\varepsilon(0)=0$. For a given electron density in a SL system, Eq. (89) gives the relationship between the electron density, n, and the appropriate Fermi energy, $\varepsilon_F(n)$. Then, P_e^s in Eq. (88) can be evaluated for a given electron density by calculating the density-dependent factors $A_1(\varepsilon_F)$ and $A_2(\varepsilon_F)$.

Finally, the result for the TSEP for the cavity case given in Eq. (51a) can be modified in a similar way as for the free-space temperature-dependent and density-dependent SE [Eqs. (88)–(90)] to obtain

$$\frac{P_e^s}{n^* P_{0c}} = A_1(\varepsilon_F)\frac{\omega_c^2}{\omega^2}\sum_{k=0}^{k_{max}}\frac{J_{2k+1}^2(\omega_0/\omega)}{(2k+1)\sqrt{1-\left[\frac{\omega_c}{(2k+1)\omega}\right]^2}} + A_2(\varepsilon_F)\frac{\omega_c^2}{\omega^2}\sum_{k=1}^{k_{max}}\frac{J_{2k}^2(\omega_0/\omega)}{2k\sqrt{1-\left(\frac{\omega_c}{2k\omega}\right)^2}}, \tag{91}$$

where P_{0c} is given in Eq. (51b). In evaluating the TSEP at finite temperatures, one has to evaluate the integrals of Eqs. (85) and (86) (for the free-space case or for the cavity case) over the full Fermi function at a finite nonzero temperature. These integrals over Fermi function are numerically available over a range of approximations and are readily tabulated.

VI. DISCUSSION AND SUMMARY

In the treatment of spontaneous emission of radiation for a *single* Bloch electron in a classical ac electric field, the TSEP for both free-field and cavity-field environments depends explicitly upon the phase quantity $\phi_z = aK_{0z} - \frac{\omega_0}{\omega}\sin\varphi$, where K_{0z} is the initial Bloch electron crystal momentum in the direction of the classical ac field and φ is the initial phase of the ac field. In treating the case where the classical ac field has an initial phase of zero, results for the free-field TSEP in Eq. (35) depend only on K_{0z}, and so can be chosen to be even or odd, depending upon choice of K_{0z} as $K_{0z} = \pm \pi/a$ at the band edge, or $K_{0z}=0$ at the band minimum, respectively. However, when band filling is in play due to a given electron density, even in the independent electron approximation, then the independent electrons fill the available states from the bottom of the SL miniband up to the Fermi level, and it is found that the TSEP is not simply dependent upon the separate even or odd harmonics alone but becomes an implicit superposition of both even and odd harmonics, dependent upon the Fermi level (or electron density) as noted in Eq. (88) for the free-space TSEP, and in Eq. (91) for cavity TSEP. As discussed in Sec. III, single Bloch electron TSEP for free-space radiation output gives rise to even or odd harmonics, depending upon initial condition on K_{0z} and with ac initial phase $\varphi=0$. Also, interesting plateau structure of ascribed to localizing is observed in the normalized TSEP when plotted versus ω_0/ω; this structure reflects the behavior of the nearest-neighbor tight-binding band model. It was observed that in the limit of free-particle energy dispersion, total spontaneous-emission probability loses the harmonic structure and goes over to the Thompson scattering result. As well, the single Bloch electron TSEP for microcavity environment is described in Sec. IV and gives rise to similar even and odd harmonic selectivity with K_{0z}; as well, the Bessel-function prefactor arising from the cavity environment allows for tuning and enhancement of the desired harmonic modes of the TSEP spectrum.

As the density-dependent effects of band filling are treated, the TSEP for free space in Eq. (88) and for microcavity environment in Eq. (91) are analyzed. Eliminating γ in Eqs. (89) and (90), and assuming for convenience that $\varepsilon(0)=0$, we graphically evaluate A_1, A_2, and n/n^* versus ε_F/Δ in Figs. 6(a) and 6(b), respectively. Further, Figs. 7(a)–7(c) include the structural behavior of the free-space TSEP with ω/ω_0 from Eq. (88) as band filling increases from $\varepsilon_F/\Delta=0.1(n/n^*=0.085)$ to $0.3(n/n^*=0.45)$ and to $0.5(n/n^*=1)$. It is seen that for low band filling, where $\varepsilon_F/\Delta=0.1$, A_1 is an order of magnitude greater than $A_2(A_2/A_1=0.08)$ so that the odd harmonic steps prevail; however, as ε_F/Δ increases forward midgap at $\varepsilon_F/\Delta=0.5$, A_1 and A_2 are of the same order of magnitude $(A_2/A_1=0.5)$, and even and odd harmonic step structure wash each other out. On the other hand, when considering the structural behavior of the TSEP in Eq. (91) for the cavity case, it is observed that the influence of the cavity to *enhance and selectively tune* to the desired harmonics of the TSEP spectrum is preserved during the band-filling process even at $\varepsilon_F/\Delta=0.5$ as indicated in Fig. 8.

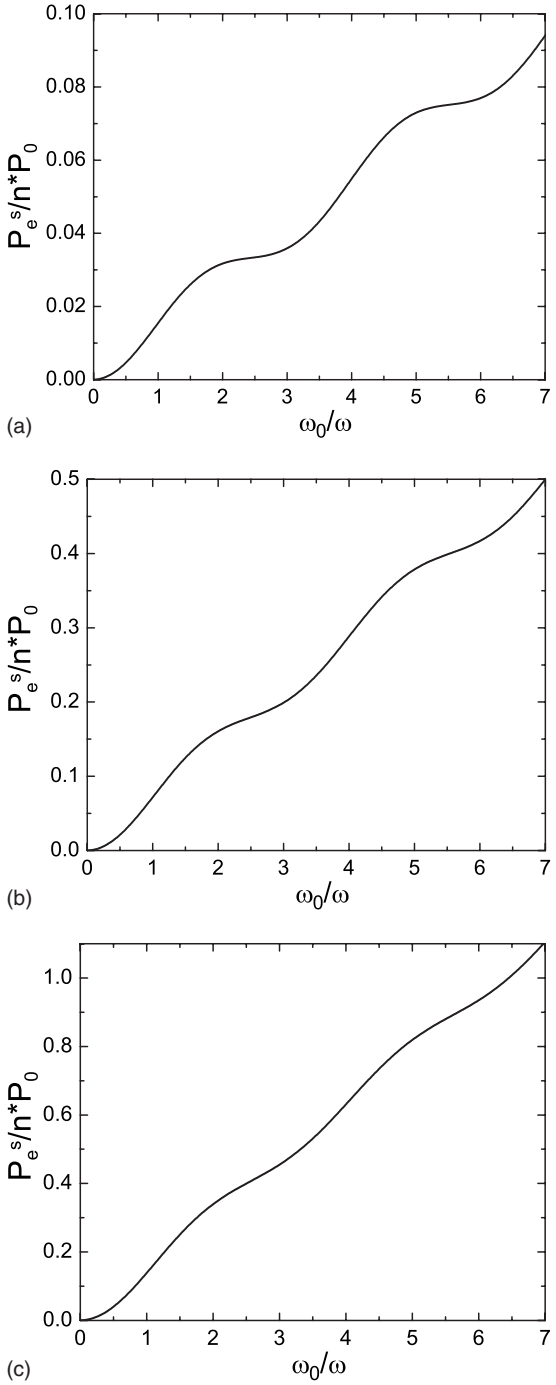

FIG. 7. Normalized total SE probability, P_e^s/n^*P_0, defined in Eq. (88) versus ω_0/ω for different values of the ratio ε_F/Δ: (a) 0.1, (b) 0.3, and (c) 0.5.

In order to demonstrate the order-of-magnitude numerical considerations for Eqs. (88) and (91), we make use of the parameters chosen for the GaAs-AlGaAs SL in previous

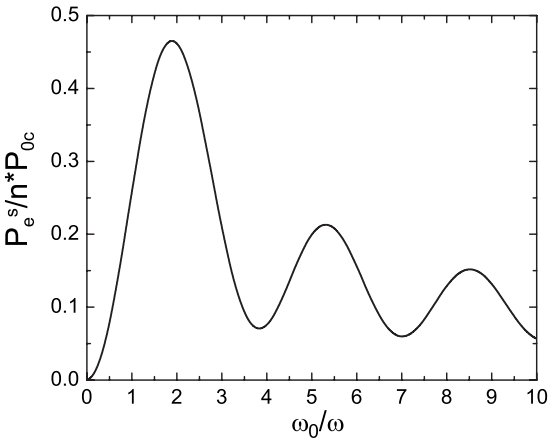

FIG. 8. Normalized total SE probability, P_e^s/n^*P_{0c}, [Eq. (91)] versus ω_0/ω for tuning of ω to the waveguide cutoff frequency, ω_c, to select the basic harmonic $\omega/\omega_c=1.1$, $\varepsilon_F/\Delta=0.5$.

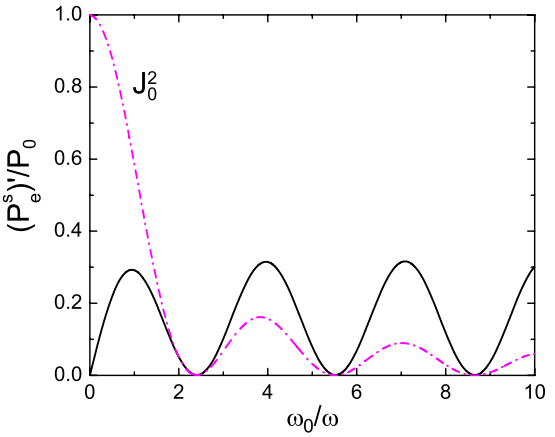

FIG. 9. (Color online) Dependences of first derivative of the normalized total SE probability [Eq. (36)], $(P_e^s/P_0)'=d[P_e^s(x)/P_0]/dx$, (solid) and squared Bessel function of zeroth order, $J_0^2(x)$, (dashed dotted) on the ratio $x=\omega_0/\omega$.

work,[23] $a=75$ Å, $\Delta=65$ meV, and $m_\perp^*=0.065m_0$. It then follows the definition of n^* below Eq. (90) that $n^*=3.7\times10^{17}$ cm^{-3}. Also, from Eq. (89), it is easy to see that when the SL lattice is empty so that $\varepsilon_F=\varepsilon(0)$, then $\gamma=1$ and $n=0$; and when it is full so that $\varepsilon_F=\varepsilon(0)+\Delta$, then $\gamma=-1$ and $n=\pi n^*$. The electron density $n=n^*$ corresponds to $\gamma=0$ such that $\varepsilon_F-\varepsilon(0)=\Delta/2$, the zero-temperature Fermi level at which the SL band is half full. From Fig. 6(a), it is noted that $A_1(n^*)=0.67$ and $A_2(n^*)=0.33$. Then the free-space TSE result of Eq. (88) gives rise to competing terms from the leading odd $J_1^2(\omega_0/\omega)$ and even $2J_2^2(\omega_0/\omega)$ terms; one finds that, for example, if one chooses $\omega_0/\omega=1.9$, which maximizes the contribution from $J_1^2(\omega_0/\omega)$, then $J_1^2(1.9)\simeq0.34$ and $2J_2^2(1.9)\simeq0.21$; thus, the odd contribution mixes nontrivially into the even component. In general, for the free-space emission, when ω_0/ω is chosen to maximize the lowest odd or even harmonic, for example, J_1^2 or $2J_2^2$, it is found that there is a significant mixing from the contiguous neighboring even or odd harmonics, $2J_2^2$ or $3J_3^2$, respectively. Therefore, one always finds a discernible mixing of even and odd neighboring components in the free-space spontaneous emission. On the other hand, for the same SL parameters, the cavity TSE result of Eq. (91) presents a separation of the even and odd components. For example, for $\omega_c/\omega=0.9(\omega/\omega_c=1.1)$, for which $J_1^2(\omega_0/\omega)/\sqrt{1-(\omega_c/\omega)^2}$ is maximum, with $A_{1,2}(n^*)$, $J_1^2(1.9)\simeq0.34$ and $J_2^2(1.9)\simeq0.1$; in this case, the odd component is much larger than the even component with negligible overlap ($\simeq3\%$). In general, for the cavity emission, when ω_0/ω is chosen to maximize a given mode, it is found that the effect of the cavity is to enhance and selectively tune the desired harmonics of the TSEP spectrum.

APPENDIX: CALCULATION OF PLATEAU POSITION

To determine the plateau position, let us calculate the first derivative of the TSEP, $(P_e^s)'=dP_e^s(x)/dx$, Fig. 9, for $P_e^s(x)$ given in Eq. (36),

$$(P_e^s/P_0)' = \sum_{k=0}^{k_{max}} 2(2k+1)J_{2k+1}(x)J'_{2k+1}(x)$$
$$= 2\cdot 1J_1(x)J_1'(x) + 2\cdot 3J_3(x)J_3'(x) + 2\cdot 5J_5(x)J_5'(x)$$
$$+ \cdots + 2\cdot(2k_{max}+1)J_{2k_{max}+1}(x)J'_{2k_{max}+1}(x), \quad \text{(A1)}$$

where $x=\omega_0/\omega$. Making use of the recurrence relations for the Bessel functions[24] in Eq. (A1), $2J'_\alpha(x)=J_{\alpha-1}(x)-J_{\alpha+1}(x)$ and $(2\alpha/x)J_\alpha(x)=J_{\alpha-1}(x)+J_{\alpha+1}(x)$, we can express the derivative of the Bessel function as $J'_\alpha(x)=(1/2)[J_{\alpha-1}(x)-J_{\alpha+1}(x)]$ and $J_\alpha(x)=(x/2\alpha)[J_{\alpha-1}(x)+J_{\alpha+1}(x)]$. Then we obtain

$$(P_e^s/P_0)' = \frac{x}{2}\{[J_0^2(x)-J_2^2(x)]+[J_2^2(x)-J_4^2(x)]$$
$$+\cdots+[J^2_{2k_{max}}(x)-J^2_{2k_{max}+2}(x)]\}$$
$$=\frac{x}{2}\{J_0^2(x)-J^2_{2k_{max}+2}(x)\}. \quad \text{(A2)}$$

For the finite interval $0<x<x_{max}$, the second term on the right-hand side of Eq. (A2) can be omitted since it takes negligibly small values with increasing k_{max} (for example, it is less than 5×10^{-13} for $0<x<10$ with $k_{max}=10$). Thus for the considered interval, we find

$$(P_e^s/P_0)' = \frac{x}{2}J_0^2(x). \quad \text{(A3)}$$

In particular, for large x ($x\gg\frac{1}{4}$), where approximately $J_0(x)=\sqrt{\frac{2}{\pi x}}\cos(x-\frac{\pi}{4})$, we obtain

$$(P_e^s/P_0)' = \frac{1}{\pi}\cos^2\left(x-\frac{\pi}{4}\right). \quad \text{(A4)}$$

Then it follows that the plateaus center is defined by the zeros of the Bessel function of the zeroth order, $J_0(x)=0$. This is bourn out in Fig. 7. Note that the second derivative $(P_e^s/P_0)''=(1/2)J_0(x)[J_0(x)+2xJ_0'(x)]$ is equal to zero at the

same x values, where $J_0(x)=0$, i.e., the center of plateau is also the inflection point of the curve $P_e^s(x)/P_0$. Similarly, for the even harmonics we can write for $P_e^s(x)$ given in Eq. (37),

$$(P_e^s/P_0)' = \sum_{k=1}^{k_{max}} 2\cdot 2kJ_{2k}(x)J'_{2k}(x)$$
$$= 2\cdot 2J_2(x)J'_2(x) + 2\cdot 4J_4(x)J'_4(x) + 2\cdot 6J_6(x)J'_6(x)$$
$$+ \cdots + 2\cdot 2k_{max}J_{2k_{max}}(x)J'_{2k_{max}}(x). \quad \text{(A5)}$$

Using the above recurrence relations, we find

$$(P_e^s/P_0)' = \frac{x}{2}\{[J_1^2(x) - J_3^2(x)] + [J_3^2(x) - J_5^2(x)]$$
$$+ \cdots + [J^2_{2k_{max}-1}(x) - J^2_{2k_{max}+1}(x)]\}$$
$$= \frac{x}{2}\{J_1^2(x) - J^2_{2k_{max}+1}(x)\}, \quad \text{(A6)}$$

or, neglecting the second term on the right-hand side,

$$(P_e^s/P_0)' = \frac{x}{2}J_1^2(x). \quad \text{(A7)}$$

In particular, for large x $(x \gg \frac{3}{4})$, we find

$$(P_e^s/P_0)' = \frac{1}{\pi}\cos^2\left(x - \frac{3\pi}{4}\right) = \frac{1}{\pi}\sin^2\left(x - \frac{\pi}{4}\right). \quad \text{(A8)}$$

Then it follows that in this case the plateaus center is defined by the zeros of the Bessel function of the first order, $J_1(x)=0$. From the second derivative $(P_e^s/P_0)''=(1/2)J_1(x)[J_1(x)+2xJ'_1(x)]$ it also follows that the center of plateau is the inflection point of the curve $P_e^s(x)/P_0$.

*Also at Department of Theoretical Physics, Institute for Semiconductor Physics, Pr. Nauki 41, Kiev 03028, Ukraine.

[1] D. H. Dunlap and V. M. Kenkre, Phys. Rev. B **34**, 3625 (1986); **37**, 6622 (1988); Phys. Lett. A **127**, 438 (1988).

[2] M. Holthaus, Phys. Rev. Lett. **69**, 351 (1992); M. Holthaus and D. Hone, Phys. Rev. B **47**, 6499 (1993); D. W. Hone and M. Holthaus, *ibid.* **48**, 15123 (1993).

[3] F. G. Bass and A. A. Bulgakov, *Kinetic and Electrodynamic Phenomena in Classical and Quantum Semiconductor Superlattices* (Nova Science, New York, 1997), p. 246.

[4] Y. O. Averkov, F. G. Bass, A. P. Panchekha, and O. M. Yevtushenko, Phys. Rev. B **48**, 17995 (1993).

[5] G. J. Iafrate, J. P. Reynolds, J. He, and J. B. Krieger, Int. J. High Speed Electron. Syst. **9**, 223 (1998).

[6] A. A. Ignatov, K. F. Renk, and E. P. Dodin, Phys. Rev. Lett. **70**, 1996 (1993).

[7] O. M. Yevtushenko, Phys. Rev. B **54**, 2578 (1996).

[8] T. Hyart, K. N. Alekseev, and E. V. Thuneberg, Phys. Rev. B **77**, 165330 (2008).

[9] L. Esaki and R. Tsu, IBM J. Res. Dev. **14**, 61 (1970); R. Tsu and L. Esaki, Appl. Phys. Lett. **19**, 246 (1971).

[10] W. L. Bloss and L. Friedman, Appl. Phys. Lett. **41**, 1023 (1982).

[11] Y. C. Chang, J. Appl. Phys. **58**, 499 (1985).

[12] J. F. Lam, B. D. Guenther, and D. D. Skatrud, Appl. Phys. Lett. **56**, 773 (1990).

[13] V. N. Sokolov, L. Zhou, G. J. Iafrate, and J. B. Krieger, Phys. Rev. B **73**, 205304 (2006).

[14] V. N. Sokolov, G. J. Iafrate, and J. B. Krieger, Phys. Rev. B **75**, 045330 (2007).

[15] J. B. Krieger and G. J. Iafrate, Phys. Rev. B **33**, 5494 (1986); G. J. Iafrate and J. B. Krieger, *ibid.* **40**, 6144 (1989).

[16] J. B. Krieger, A. A. Kiselev, and G. J. Iafrate, Phys. Rev. B **72**, 195201 (2005).

[17] W. Heitler, *The Quantum Theory of Radiation* (Dover, New York, 1954), p. 34.

[18] For $\omega_q = c\,q$, this corresponds to neglecting a small term $\sim v_\perp/c$ as compared to unity.

[19] Although the selection rule of Eq. (16) denotes that $q_{max}=m\omega/c$ should go to infinity, the explicit convergence behavior of the sum due to the rapid mathematical decay of the coefficients with physical argument, ω_0/ω, naturally truncates the need to carry the series sum past several terms. This is clearly noted in Figs. 1(b) and 2(b).

[20] For nearest-neighbor tight binding, where electron energy dispersion can be written in the form of Eq. (28), the electron velocity component $\mathbf{v}_\perp(\mathbf{k}_0)=\mathbf{v}_\perp(\mathbf{K}_\perp)=(1/\hbar)\nabla_{\mathbf{K}_\perp}[\varepsilon_\perp(\mathbf{K}_\perp)]$ is independent of time; then the probability amplitude in Eq. (13) is evaluated as $A^{(e)}_{\mathbf{q},j}(\mathbf{k}_0,t)=\frac{iD}{m\omega\sqrt{q}}[e^{-im\omega\tau}-1]\mathbf{v}_\perp\cdot(\hat{\varepsilon}_{\mathbf{q},j})_\perp=0$, where the use has been made of the selection rule $\omega_q=m\omega$.

[21] G. Gallot, S. P. Jamison, R. W. McGowan, and D. Grischkowsky, J. Opt. Soc. Am. B **17**, 851 (2000).

[22] N. Marcuvitz, *Waveguide Handbook* (Peregrinus, London, 1993).

[23] L. Friedman, J. Phys. C **17**, 3999 (1984).

[24] G. N. Watson, *A Treatise on the Theory of Bessel Functions*, 2nd ed. (Cambridge University Press, Cambridge, England, 1966), p. 45.